Bulletin of the Mineral Research and Exploration

http://bulletin.mta.gov.tr

Determination of structural characteristics of Tuzgölü Fault Zone using gravity and magnetic methods, Central Anatolia

Bahar DİNÇER[a*] and Veysel IŞIK[b]

[a]*Turkish Petroleum Corporation, TR-06530, Ankara, Turkey*
[b]*Ankara University, Department of Geological Engineering, Tectonics Research Group, TR-06830, Ankara, Turkey*

Research Article

Keywords:
Geophysical method, Downward continuation, Tuzgölü Basin, Fault Zone, Central Turkey.

ABSTRACT

The anomaly maps and amplitude and wavelength changes of the anomalies obtained from gravity and magnetic methods can provide to identify fault traces in the underground. The Tuzgölü Fault Zone (TFZ), the NW-SE striking active fault zone in central Anatolia, includes fault strands that cut the basement and basin deposits. Our magnetic and gravity analysis suggests that Tuzgölü Basin and its surroundings are characterized by distinct depression and ridge areas. Gravity anomaly data show the presence of faults at depths of sea level (0 m), -1000 m, -2000 m, -3000 m, and -4000 m. These faults are mostly normal and reverse faults, as well as the lesser amount of vertical faults (high-angle normal/reverse faults) with NW-SE, N-S, and NE-SW-striking. The normal faults are of the structural development and the deposition of the Tuzgölü Basin units, which occurred late Cretaceous-Middle Eocene and Early Miocene-Quaternary Periods. The reverse faults originated from the result of the regional-scale compressional regime during Middle Eocene-Late Oligocene/ Early Miocene based on the fault dating data from the literature. The active TFZ, including several fault strands, are relatively younger faults in the region that have initiated to develop during faulting events from after Middle Miocene or Early Pliocene.

Received Date: 30.05.2019
Accepted Date: 18.12.2019

1. Introduction

Gravity and magnetic methods are natural potential methods that have been performed for many years in the subsurface surveys. They have been used extensively, especially in oil and gas researches, since the beginning of the 20th century (Reynolds, 2011). Among the critical problems encountered in the studies related to subsurface geology, determination of buried faults, determination of the locations, characteristics (e.g., geometry, type, amount of throw) of buried and surfaced faults, as well as the determination of geological contacts are prominent. Natural potential methods are among the geophysical methods used to understand these discontinuities. Accordingly, gravity and magnetic measurements and anomalies obtained to enable the determination of faults in shallow sections of the continental crust, mapping these structures and determining their characteristics.

Horizontal and vertical changes in density and magnetization show the transition between different geological units, and this situation appears as an anomaly in the maps (Wilcox, 1974). In this context, there are studies in the literature that use derivative-based algorithms to identify anomaly exchange lines (Boschetti, 2005; Cooper and Cowan, 2008; Hosseini et al., 2013), such as the total horizontal derivative

Citation info: Dinçer, B., Işık, V. 2020. Determination of structural characteristics of Tuzgölü Fault Zone using gravity and magnetic methods, Central Anatolia. Bulletin of the Mineral Research and Exploration 162, 145-174. https://doi.org/10.19111/bulletinofmre.661245

* *Corresponding author: Bahar DİNÇER, badincer@tpao.gov.tr*

(Cordell and Grauch, 1982; 1985; Lyatsky and Dietrich, 1998), boundary determination (Blakely and Simpson, 1986), analytical signal (Roest et al., 1992), tilting signal derivative (Miller and Singh, 1994; Salem et al., 2008) and total horizontal tilting angle derivative method (Verduzco et al., 2004). Images created with the total horizontal derivative technique are important in determining the linearities representing discontinuities, understanding lateral changes in lithologies and interpreting some other structural formations (Saad, 2006; Cooper and Cowan, 2008; Aydoğan, 2011; Zhang et al., 2011; Hosseini et al., 2013).

The Central Anatolian Region, which also includes the study area, is among the areas where gravity and magnetic methods are successfully applied to understand the underground lithology and structural features (Uğurtaş, 1975; İlkışık et al., 1997; Aydemir and Ateş, 2006*a*; 2006*b*; 2008; Aydoğan, 2011; Oruç, 2011). Tuzgölü Basin and its surroundings in the region are home to many fault zones (Dirik and Göncüoğlu, 1996; Koçyiğit, 2003; Özsayın and Dirik, 2007; Özsayın et al., 2013; Işık et al., 2014). Although the morphological features of TFZ and the contact relationship between Quaternary-Holocene sediments and old units are evident, the character and age of the fault zone is a subject of discussion in the literature.

This study aims to reveal the deep characteristics of the TFZ, which is located in the northeastern part of the Tuzgölü basin and has an active fault zone, with the help of gravity and magnetic methods. In this context, the TFZ study area includes Kırşehir, Aksaray, Karaman, Adana sections of Active Fault Map of Turkey prepared and printed by the MTA (Emre et al., 2011). The northwest-southeast trending fault zone consists of several fault strands with different orientations and spread. To reach the aim of the study, firstly gravity and magnetic properties of a vast region including TFZ were determined, then the fault trace of the TFZ and its immediate surroundings at sea level (0 km), -1000 m, -2000 m, -3000 m and -4000 m depths were interpreted. With this study these are aimed; (1) determination of fault traces up to 4 km depth in TFZ and its near surroundings, (2) preparation of the map showing fault traces in 6 areas where faulting is typical along the zone, and determination of fault characteristics from individual sections of the areas, (3) demonstration of the descriptive/interpretive geometries of the faults on the vertical plane, and (4) evaluation of the TFZ in the light of the obtained findings and data from the literature.

2. Tuzgölü Basin

Central Anatolia region is characterized by paleotectonic units that are Sakarya Zone, Kırşehir Block/Menderes-Taurus Platform, and İzmir-Ankara-Erzincan Suture Zone. Although controversial, the Inner-Taurus Suture Zone is another paleotectonic unit in the region. (Şengör and Yılmaz, 1981; Okay and Tüysüz, 1999) (Figure 1). The region consists of different lithologies, both continental and oceanic crust affinity. Metamorphics, ophiolitic rocks, granitoids and volcanic rocks, and sedimentary rocks are the occuring type of lithologies (Göncüoğlu et al., 1992; Tüysüz et al., 1995; Poisson et al., 1996; Görür et al., 1998; Seyitoğlu et al., 2000; Yalınız et al., 2000; Whitney et al., 2001; Kaymakçı et al., 2003; Işık et al., 2008; 2014; Keskin et al., 2008; Lefebvre et al., 2011; Özsayın et al., 2013; Gülyüz et al., 2013).

The Tuzgölü Basin is one of the Central Anatolian Basins that is formed in Anatolides in the paleotectonic classification of Turkey by Ketin (1966) or the Anatolide-Tauride platform classified by Şengör and Yılmaz (1981) and Okay and Tüysüz (1999). The basin might be a fault-controlled basin developed in the Kırşehir Block of the paleotectonic period and the Anatolian Plate of the neotectonic period of Turkey (Figure 1). Görür et al. (1984) define Tuzgölü Basin as the forearc basin that develops between Kırşehir arc and Inner-Taurus Suture Zone. The Central Anatolian Basins, including the Tuzgölü Basin, are divided into three groups (magmatic arc-related basins, collision-related peripheral arc-front basins, and sedimentary cover basins) according to their tectonic location, structural and stratigraphic features by Görür et al. (1998); the Tuzgölü Basin is defined as the magmatic arc associated basin.

Stratigraphical and sedimentological features of the Tuzgölü Basin are well-known with the evidence of paleontological findings (Rigo de Righi and Cortesini, 1960; Arıkan 1975; Ünalan and Yüksel, 1978; Görür et al., 1984; Derman et al., 2003; Dirik and Erol, 2003). The basin is northwest-southeast trending in terms of its present geometry. The Haymana Basin is located in the northwest extension of the Tuzgölü basin, and the Ulukuşla Basin is located in the southeast

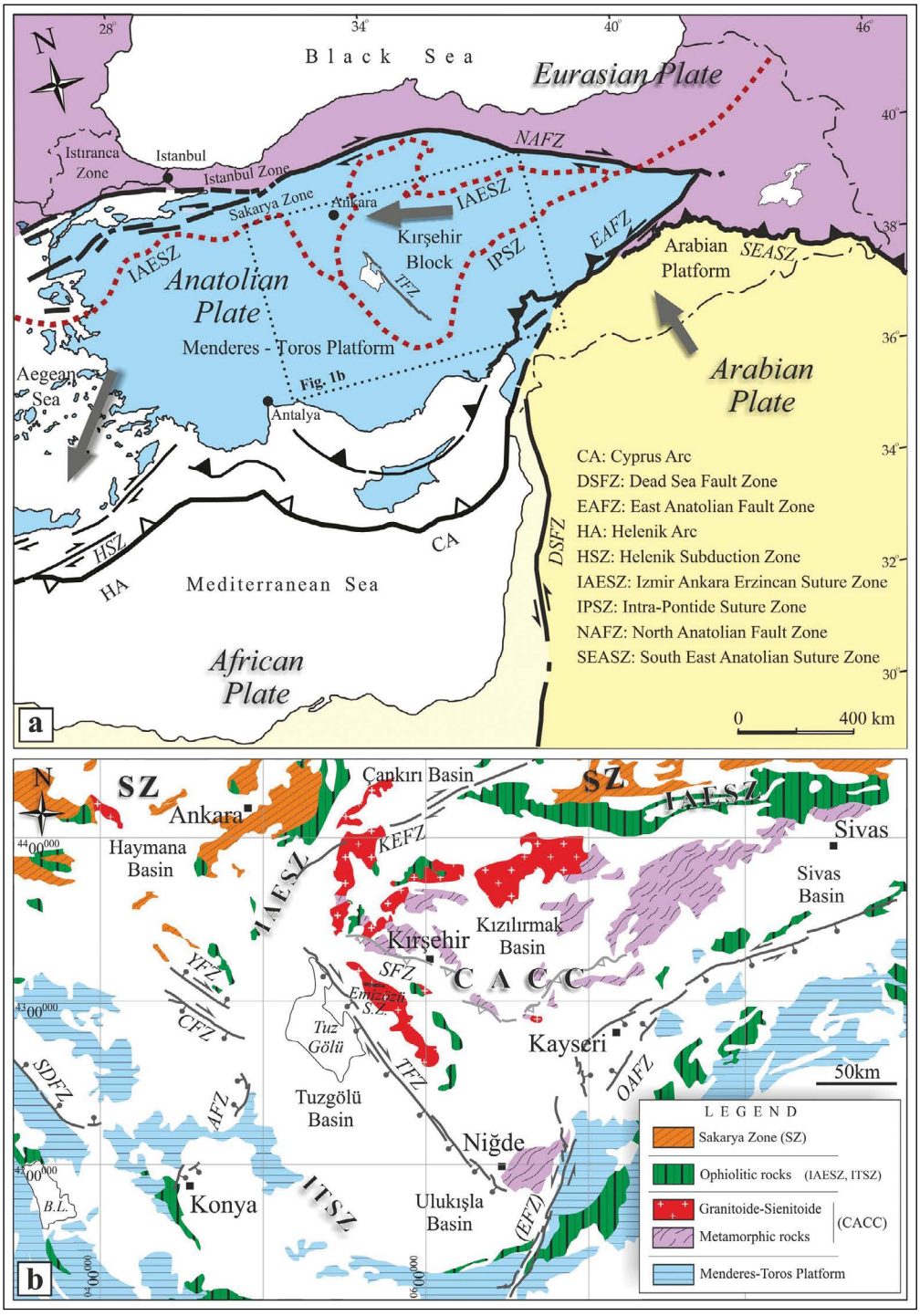

Figure 1- a) Map showing the main tectonic features of Turkey and surrounding area and regional plate boundaries of the Alpine-Himalayan orogeny (Redrawn from Işık et al., 2014) and b) simplified geological map of the Central Anatolia (Modified from Işık et al., 2008; 2014). Some of the faults are drawn from the Emre et al., 2011 Active Fault Map of Turkey. *Abbreviations:* AFZ: Altınekin Fault Zone, BG: Beyşehir Lake, CFZ: Cihanbeyli Fault Zone, EFZ: Ecemiş Fault Zone, IAEKZ: Izmir-Ankara-Erzincan Suture Zone, ITKZ: Intra-Tauride Suture Zone, KEFZ: Kırıkkale-Erbaa Fault Zone, OAFZ: Orta Anadolu Fault Zone, OAKK: Central Anatolian Crystalline Complex, SZ: Sakarya Zone, SFZ: Savcılı Fault Zone, SDFZ: Sultandağ Fault Zone, TFZ: Tuzgölü Fault Zone, YFZ: Yeniceoba Fault Zone.

extension of it (Figure 1b). Görür et al. (1984) divided the Tuzgölü Basin into two sub-basins and called Tuzgölü and Haymana sub-basins, although known the Tuzgölü and Haymana Basins in present literature, respectively. The eastern part of the Tuzgölü Basin is bordered by the Kırşehir Massif / Central Anatolian Crystalline Complex rocks, while the western part is bordered by the Bolkar unit / Inner-Taurus Ocean / Kütahya-Bolkardağ metamorphics / Afyon Zone rocks (Menderes-Tauride Platform) (Figure 1b).

Basin stratigraphy consists of two main lithology groups. These are basement rocks and basin units. The Central Anatolian Crystalline Complex commonly exposed, especially in Kırşehir and its surroundings, occurs in the eastern part of the basin. It includes metamorphites, granitoid rocks, and ophiolitic melange rocks (Seymen, 1984; Göncüoğlu and Türeli, 1993; Köksal et al., 2004; Işık, 2009; Işık et al., 2014) (Figure 2). The western part of the basin is represented by the metamorphic rocks of the Bolkar Unite and the ophiolitic rocks remnant of the Izmir-Ankara ocean (Karaman, 1986; Göncüoğlu et al., 1996; Eren, 2003*b*). These lithologies are considerably overlain by young units. Ophiolitic rocks characterize the basement rocks in the northern part of the basin. The ophiolitic rocks also separate the Tuzgölü Basin and Haymana Basin and constitute the primary lithology of the basement of both basins (Görür et al., 1984; Rojay, 2013). Göncüoğlu et al. (1996) interpreted that all these ophiolitic rocks constitute the Central Anatolian Ophiolites, and are a product of accretionary prism that occurred during the closure process of the Izmir-Ankara Ocean.

Stratigraphy of the Tuzgölü Basin is well-known, although there is a controversy (Turgut, 1978; Dellaloğlu and Aksu, 1984; Görür et al., 1984; Ulu et al., 1994; Göncüoğlu et al., 1996; Derman et al., 2003; Dirik and Erol, 2003). The basin units are divided into three rock groups based on sediment characteristics and the main unconformity surface of the basin units. These are Late Cretaceous-Cenozoyic units, Oligo-Miocene units, and Plio-Quaternary units (Figure 3). Late Cretaceous-Cenozoyic units of Tuzgölü Basin are mostly overlain by young units. Widespread outcrops of the Late Cretaceous-Cenozoyic units are seen in the eastern part of the basin. Data from some deep drilling wells in different parts of the basin contributed to the forming of basin stratigraphy. The western and eastern parts of the basin show distinctive differences in terms of the spread of lithologies and facies characteristics (Görür et al., 1984; Derman et al., 2003; Dirik and Erol, 2003; Özsayın and Dirik, 2007; Gürbüz, 2012; Kürçer, 2012; Göksu, 2015) (Figure 3).

The southeastern part of the basin is covered by Miocene-Quaternary/Holocene volcanic rocks, which the area in literature is defined as Cappadocia Volcanic Region (Beekman, 1966; Ercan et al., 1992; Aydar et al., 1994; Deniel et al., 1998; Toprak, 2003; Schmitt et al., 2014). Volcanoes such as Karacadağ, Kötüdağ, Keçikalesi, Hasandağ, Keçiboyduran, and Melendiz are volcanoes that have had activity at different intervals in this period. Keçikalesi caldera is the oldest volcanic complex with 12.4-13.7 Ma (K-Ar method: Besang et al., 1977). Hasandağ caldera is a multi-caldera complex (Beekman, 1966; Aydar and Gourgaud, 2002). U-Th zircon dating method reveals that Hasandağı volcano was active during the Holocene period (6960 ± 640 BC: Schmitt et al., 2014). The Keçiboyduran and Melendiz volcanoes in the east have similar features and are interpreted as Early Pliocene (Toprak, 2003).

All these basin units reveal that Tuzgölü Basin has a thick sedimentary and volcanic sequence. Data from deep drilling wells show more than 4 km of a structural thickness of basin units in some areas (e.g., Bezirci-1 Well). Aydemir and Ateş (2006*b*) determined the deepest part of the Haymana and Tuzgölü Basins using the basin modeling of the gravity and magnetic data with some assumptions. The density of the metamorphic rocks forming the basement rocks of the basins and the basin units are conceded 2.65 gr/cm^3 and 2.40 gr/cm^3, respectively. According to these researchers, different parts of Tuzgölü Basin have varying depths and can reach a depth of 12-13 km.

3. Tuzgölü Fault Zone (TFZ)

The geological structures in the Central Anatolia to be differentiated as paleotectonic and neotectonic periods are widely accepted. The faults that occurred during the paleotectonic period are related mainly to the obduction of ophiolitic rocks. Ophiolitic rocks with different sizes and geometries overlie Mesozoic and Lower Cenozoic units with tectonic contact. These faults can be seen in limited areas uncovered by young rock units in the region. Emizözü shear zone, defined

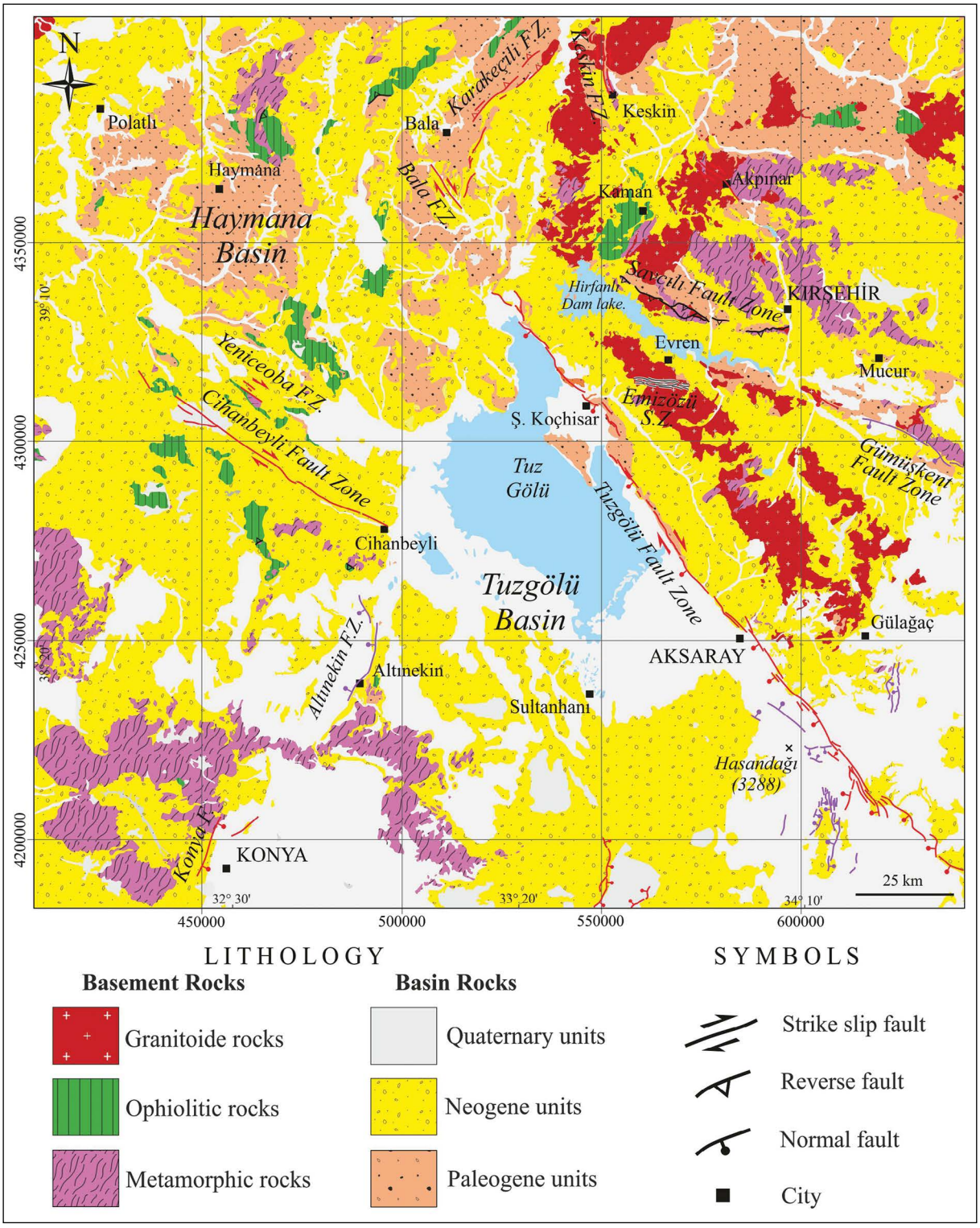

Figure 2- Simplified geological map of the Tuzgölü basin and surrounding area (Modified from MTA-2002 1:500.000 scale Geological Map of Turkey - Ankara, Kayseri). Active faults with red and violet-colored adopted from MTA-2011 Active Faults Maps of Turkey. Emizözü Shear Zone and Savcılı Fault Zone adopted from Işık, (2009) and Işık et al. (2014), respectively.

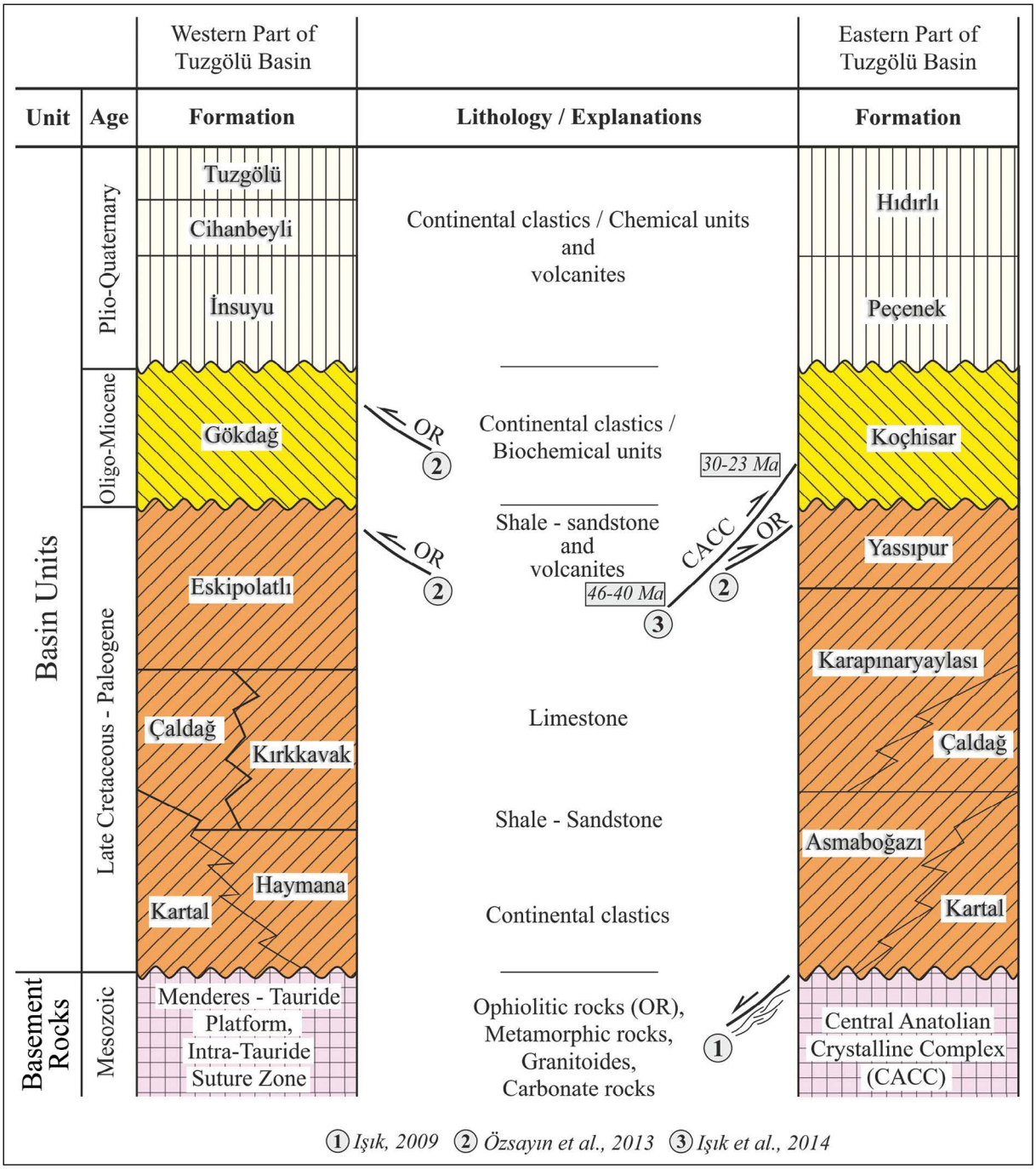

Figure 3- Correlation of the simplified stratigraphic columns of the western and eastern parts of the Tuzgölü Basin. (Modified from Dirik and Erol, 2003).

by Işık (2009), occurred during the Upper Cretaceous extensional regime, represent the structure of the paleotectonic period in the region. The Savcılı Fault Zone with well-constrained age is a regional-scale fault zone formed between middle Eocene and late Oligocene, which is another essential paleotectonic structure (Çağlayan, 2010; Işık et al., 2014). According to Çağlayan (2010) and Işık et al. (2014), the Savcılı Fault Zone is characterized by reverse/thrust faults due to compression regime. There are also studies suggesting that the zone might be occurred tectonic regime either extensional regime (Yürür and Genç, 2006) or lateral compressional regime (Lefebvre et al., 2013; Gürer and van Hinsbergen, 2019).

Central Anatolian Fault Zone, Niğde Fault Zone, Konya-Blok Fault Zone/Altekin Fault Zone, Tuzgölü Fault Zone (TFZ), İnönü-Eskişehir Fault Zone (System) and Akşehir Fault Zone are NW and NE trending, which are important fault zones of the neotectonic period (Dirik and Erol, 2003; Eren, 2003*a*; Koçyiğit, 2003; Özsayın and Dirik, 2007; Işık, 2009; Kürçer, 2012; Fernandez-Blanco et al., 2013; Özsayın el al., 2013).

The Tuzgölü Fault Zone (TFZ) is an NW-SE trending intra-continental fault zone. The TFZ is first shown as a lineament in the tectonic map by Edmund Naumann (1896). In geology based-studies, the zone is described in not only different names but also its fault characteristics. For example, According to Koçyiğit (2003), the TFZ extend between Paşadağı (Ankara) and Bor (Niğde) and has approximately 220 km in length and range between 15 and 25 km in width. Furthermore, the same zone is 190-200 km long and 5-25 km wide, as suggested by Dirik and Erol (2003). The length of the TFZ is about 195 km if we consider fault traces in MTA-Active Fault Map. The width of the zone displays significant local differences because of the distribution of the fault traces along the TFZ. Changing the width of the TFZ is related to fault geometries such as bending, step-over, or networks of fault splays. The southwest extension of the zone, especially from Aksaray, is approximately 25 km in width, while other parts of it vary between 1 km and 5 km.

Although the present structure of the TFZ appears to be geological fault contact between Plio-Quaternary deposits and older basin rocks and/or cutting them, fault characteristic and age of faulting is a matter of debate. Şaroğlu et al. (1987) suggest that the TFZ is a high-angle reverse fault component right-lateral strike-slip faulting. According to Dirik and Erol (2003), the fault zone is represented by steps, sub-parallel faults with half-graben, or horst-graben morphology. Dirik and Göncüoğlu (1996) paid attention to the presence of deformed alluvial fans, fault scarps in downthrown western block, and clockwise rotation of stream beds on the eastern block of the main fault. Toprak and Göncüoğlu (1993), and Toprak (2003) suggest that southern part of the TFZ display parasitic cone arrays and volcanic activity, hot springs and travertines, fault-controlled terrace developments and some markers (e.g., displaced lava flows) representing right-lateral faulting. Koçyiğit (2003) mentioned that the TFZ is conjugate of the Central Anatolian Fault Zone, and shows the right lateral fault zone with a significant amount of a normal component. Kürçer (2012) and Kürçer and Gökten (2014) divided the TFZ into 11 fault segments with ranging from 9 km to 30 km longs. In these studies, the amount of normal displacement of the zone from the Pliocene to the present was calculated as 230-290 m. These researchers also suggest that the TFZ is an oblique normal fault zone. Derman et al. (2003) suggested that the zone initially acts as a normal fault character and later left-lateral strike-slip fault character during Eocene; in the following period again, it was acted like a normal fault.

Some of the researchers consider the starting age of the TFZ as Late Cretaceous (Uygun et al., 1982; Görür et al., 1984; Çemen et al., 1999; Fernandez-Blanco et al., 2013). Ages of the post-Maastrichtian (Derman et al., 2003), Eocene (Arıkan, 1975) and Miocene (Dellaloğlu and Aksu, 1984) are also recommended for the occurrence of the TFZ. Işık (2009) documented that the Tuzgölü Basin developed during extensional tectonics coexisting with a ductile shear zone and related with normal faulting in the late Cretaceous, which present morphology of the TFZ is characterized by post-Miocene faulting. Koçyiğit (2003) and Kürçer (2012) argue that the TFZ is at a post-Early Pliocene age, which some segments of the zone is also seismically active. The relative activity of the TFZ during Quaternary was documented by Yıldırım (2014) using morphometric index data.

4. Method and Findings

4.1. Method

Gravity and magnetic methods are fundamental geophysical methods. In use, it is necessary to obtain a large number of measurements in a short period of time and be relatively low cost. That is why both methods are widely used for economic purposes (e.g., petroleum-natural gas, mineral, geothermal fields) as well as exposing underground geology (e.g., crust thickness, basin or basement elevation areas, sediment thickness, volcanic propagation, salt domes, other geological structures) (Telford et al., 1990; Soengkono, 1999; Reynolds, 2011). These methods also are frequently used in the detection of ancient

objects buried underground and in areas performed seismic studies where the image quality is not good enough.

Density in the gravity method and magnetization in the magnetic method creates potential field anomalies in measurements (Wilcox, 1974). The maximum and minimum values of the primary or secondary derivatives of the potential area are used to determine the source causing the anomaly that occurred during sudden changes in density or magnetization and to find the boundaries of the structure (Cordell, 1979; Pınar, 1984). To identify the geological formations causing this anomaly, horizontal and vertical derivatives of the potential area is preferred by many researchers (Cordell, 1979; Cordell and Grauch, 1985; Miller and Singh, 1994; Aydın, 1997; Verduzco et al., 2004; Cooper and Cowan, 2008; Aydoğan, 2011). The potential field method provides the ability to take derivatives in horizontal (x, y) and vertical (z) directions using the available data (Saad, 2006). Derivatives taken in the horizontal direction reveal the discontinuities, while the derivative taken in the vertical direction reveals the depth and spread of the source. Isostatic gravity maps, which are balanced by removing their continental effects, also include the total effect of deep and shallow structures like Bouguer gravity maps. Regional anomalies refer to deep structures, and residual anomalies refer to shallow structures. Regional and local anomalies should be separated from each other to make the interpretation more accurate. In this study, firstly, isostatic gravity values are divided into local and regional anomalies. Low pass filter is applied to isostatic gravity anomalies up to 4 km depth for each kilometer depth from sea level. Horizontal derivative grids in x-direction were calculated for each depth on the maps obtained. Fault traces were determined on these grid maps with the help of positive and negative anomalies. Separate color is used in drawing the fault traces determined for each depth.

Gravity values can generally be measured on the ground or in the air, reduced to sea level, and interpreted at this level; however, in some cases, it can be moved to different planes for interpretation purposes (Oruç, 2013). In this methodical study called up and down extension, both temporal and spatial environment can be preferred (Pick et al., 1973; Huestis and Parker, 1979). Thus, it is possible to differentiate the anomalies caused by the geological structures and the sources that constitute the anomalies (Blakely, 1995). The amplitude and wavelength variations of the gravity and magnetic anomalies, and the depth with the lithology, respectively, can be estimated. A similar situation is applied in determining the faults affecting these lithologies. Maximum and minimum changes of gravity anomalies help us in determining the types of faults (e.g, Telford et al., 1990; Yüksel, 2011; Lowrie, 2007). The locations of the blocks formed as a result of faulting and the slope angles of the fault plane provide the opportunity to make inferences from the changes in gravity fault anomalies. Accordingly, it is possible to understand whether faulting from gravity fault anomalies is close to vertical or less than 90° inclined. More importantly, it is possible to determine whether the inclined plane faulting is of normal or reverse fault character. Mathematical relations about these are given by Telford et al. (1990).

Air magnetic data obtained from MTA General Directorate was used for total magnetic (air magnetic) field data of the region, especially the TFZ, which is the subject of the study. These data were obtained between 1978-1989 at the height of 600 m in the region and with a profiled interval of approximately 1-5 km; data were re-grided with 5x5 km intervals and then 1x1 km. Magnetic anomaly map was created by applying the correction of - the International Geomagnetic Reference Area (IGRF-1985) - with an algorithm developed by Baldwin and Langel (1993) (Ateş, 1999). After the IGRF corrections have been made taking into account the measurement dates, the data has been reduced to the magnetic pole in order to eliminate magnetic deviations, to facilitate the interpretation and to eliminate the complexity of the process and to ensure that the anomaly is located on its actual location (Blakely, 1995). Then 600 m down extension was applied.

Gravity data were obtained from Turkish Petroleum (TPAO). In the region, including the study area, measurements were made at approximately 120,000 station points with the gravimeter device, and these data were recorded. Within the scope of this study, tool drift, latitude, free air, Bouguer plate, topographic correction, sea surface reduction, and isostasy corrections were applied to the obtained raw data. In the Bouguer calculation, the reduction density is 2.20 gr/cm^3 in the topographic correction, the density values of 2.20 gr/cm^3 are used. Oasis Montaj 2007 software was used for all corrections, and afterward,

since it is necessary to work in a wide area, isostatic gravity values balanced by removing deep continental effects were mapped, and subsequent operations were performed using these values.

4.2. Findings

Figure 4a displays the air magnetic anomaly map that is formed for the broad region, including the TFZ. The map shows the total effect of anomalies from

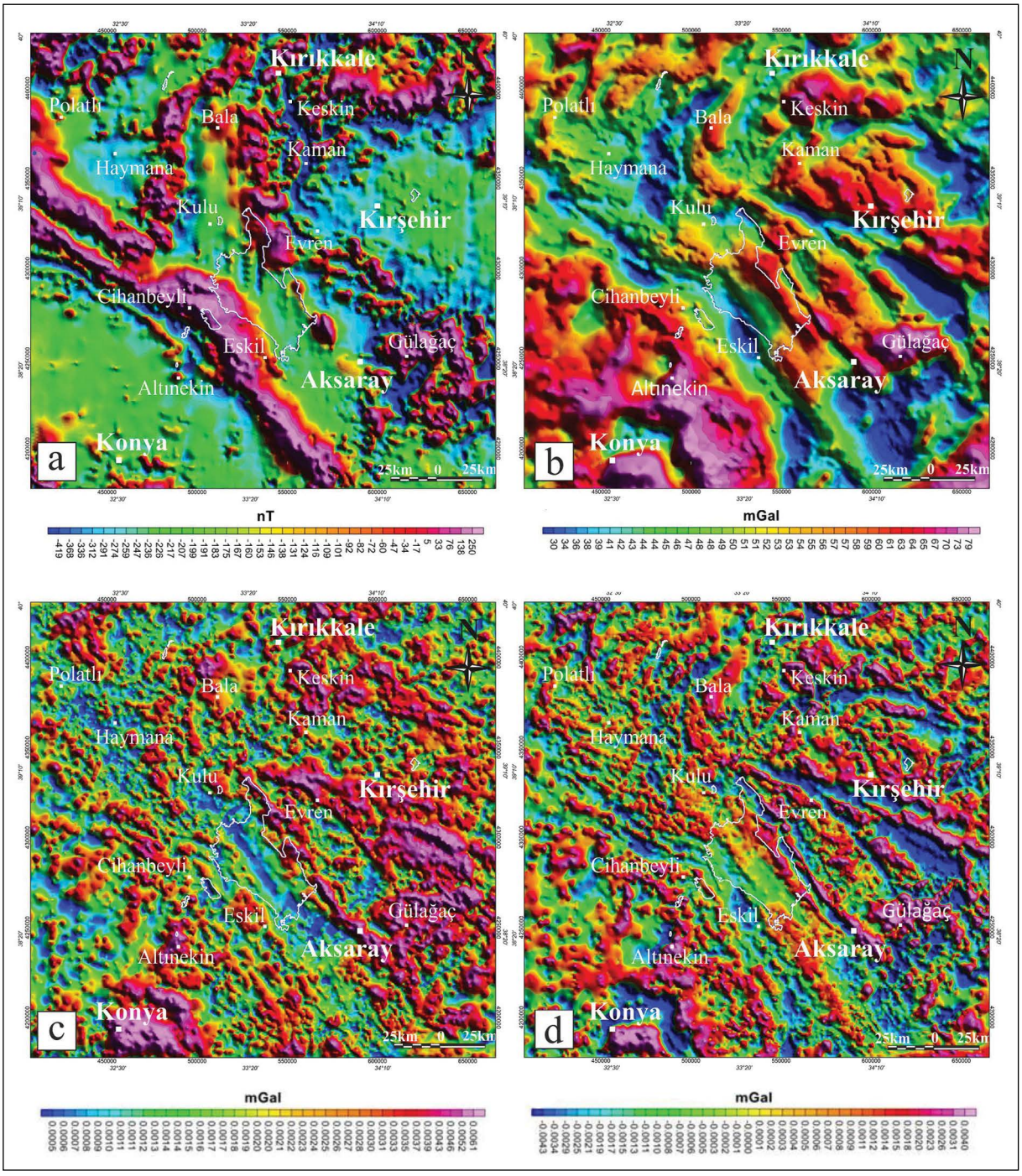

Figure 4- a) Aeromagnetic anomaly map (Contour interval was taken as 50 nT), b) isostatic gravity map (Contour interval was taken as 5 mGal), c) analytic signal map of the isostatic gravity data, and d) vertical derivative map of the isostatic gravity data.

lithologies of different depths. In the map where the contour interval is taken as 50 nT, especially the areas formed by positive anomalies of 85 nT and above are quite remarkable. These areas are represented by red and pink colors or their shades (Figure 4a). The areas with high anomaly values indicate the presence of magnetic susceptibility and/or lithologies with density. Therefore, the areas seen in the pink-red color range on the map have high magnetic susceptibility values. The areas where colors from yellow to green indicate that these parts have low magnetic susceptibility values. The areas colored in blue on the map refer to the areas where the magnetic susceptibility value is little or no according to the surrounding rocks. The isostatic gravity map for the region is given in figure 4b. The map shows the total effect of lithologies of different depths and distinct densities. In the map, the areas pink-purple in colors indicate the lithologies with high-density and blue-colored sections of the map show the lowest density lithologies.

Gravity and magnetic maps reveal where and how negative and positive anomalies are located in the region (Figures 4a, 4b). Correlation of simplified gravity and magnetic maps allow the depths of the rock units forming the anomaly in the map area (Figure 5). This comparison enables us to deduce the location and geometry of basins (e.g., Tuzgölü,

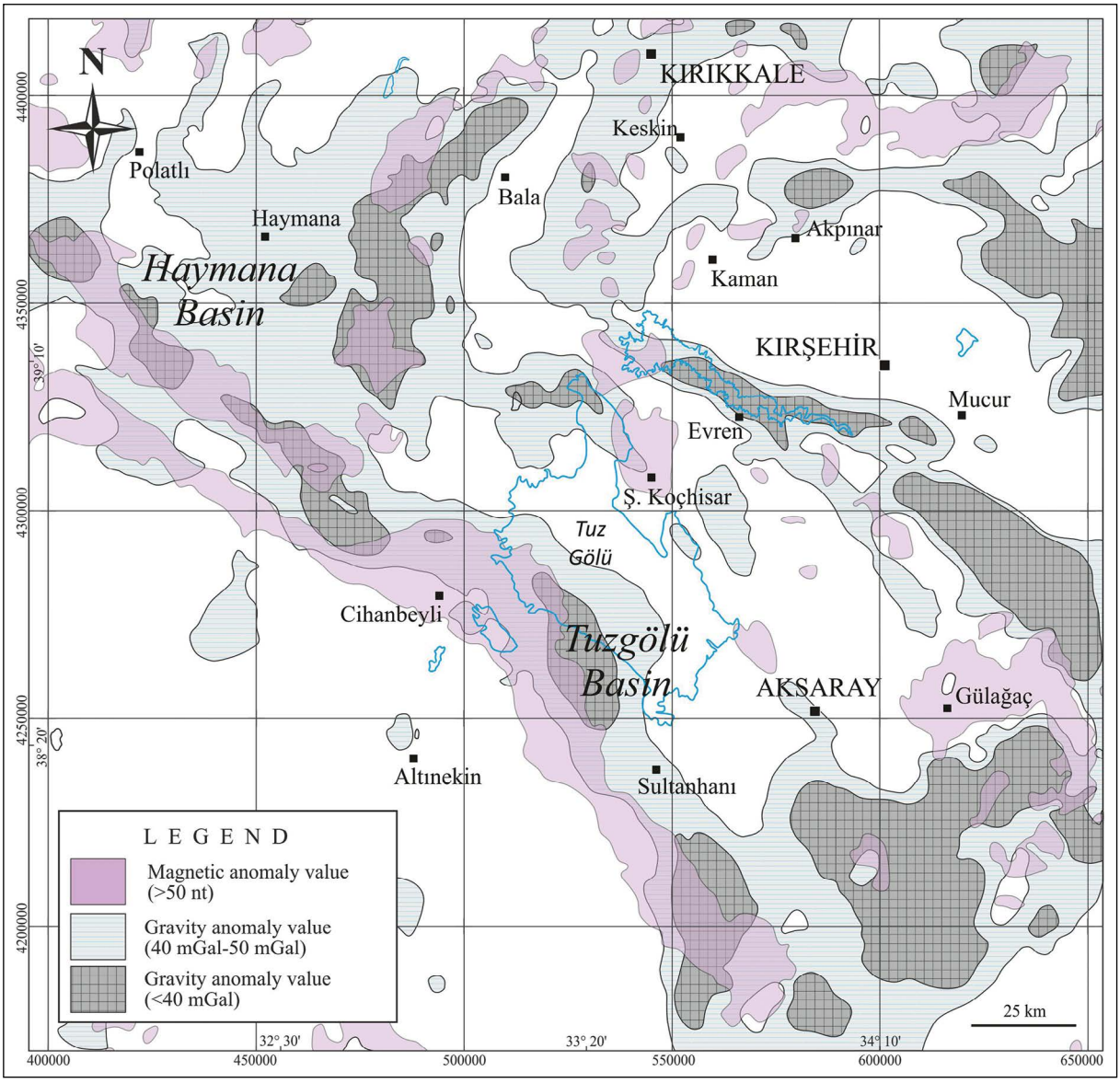

Figure 5- Map showing comparative magnetic and gravity anomalies data of the Tuzgölü Basin and its surroundings.

Haymana) and the extension of the basement units. Correlation of these data with surface geology reveals some compatibility and differences. The anomalies in gravity and magnetic maps indicate that the faultings in the region are mostly NW-SE-trending, but in the limited areas, it shows N-S orientation. The long-wavelength positive anomaly in the magnetic map with the NW-SE orientation is of deep origin and possibly represents the suture belt.

Figures 4c and 4d display maps of analytical signal and vertical derivative generated from gravity data. These maps allow us to interpret the anomalies in the map of isostatic gravity in detail. From both maps (analytical signal, vertical derivative), it can be interpreted whether the basin units in the region are too thick or how shallow the basin depths are (Figure 4c, 4d). It is essential to evaluate the positive/negative anomaly areas on the analytical signal map together with the anomaly areas on the gravity map. Areas with positive anomalies in the analytical signal map and areas with similar anomalies in the isostatic gravity map show that the units that make up this anomaly are located close to the surface or on the surface. Again, the positive/negative anomaly areas in the vertical derivative maps allow the understanding of how deep or shallow the units are. This fact is as possible as for faults.

In determining the basement rock depth for the Tuzgölü Basin and its surroundings, a graph (Figure 6) prepared with the depth estimation technique (Yüksel,

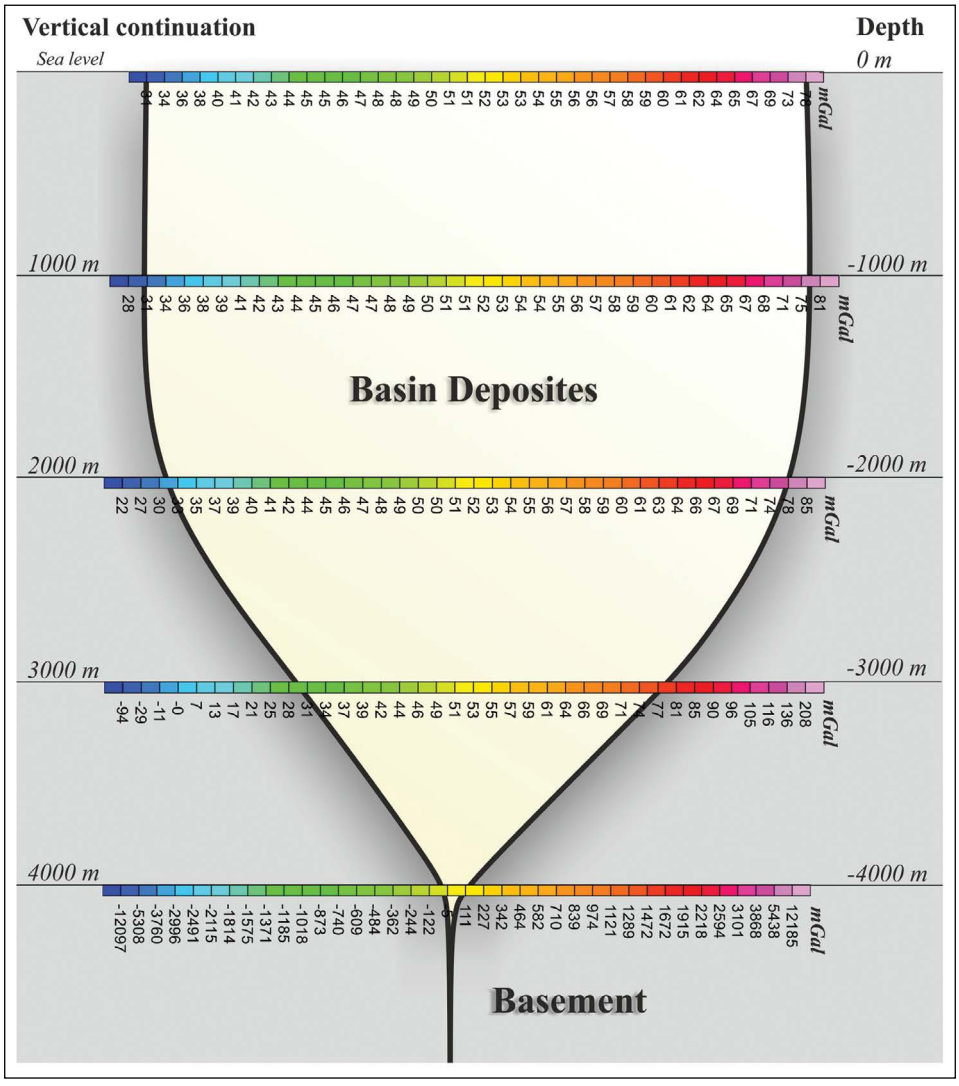

Figure 6- Estimation graphic showing regional depths of basement rocks using the downward continuation maps of the Tuzgölü Basin and its surroundings.

2011) and power spectrum graphics (Figure 7) were made. In this context, downward continuation maps (Sea level, -1000 m, -2000 m, -3000 m, and -4000 m) have been prepared to determine how deep the basement rock buried in the region is located from the sea level.

The estimation graph from the downward continuation map values created for every -1000 m from the sea level up to -4000 m is given as figure 6; The estimation graph shows the average rock depths entered in the base rocks in the region. The downward continuation map created for sea level reveals that the border between low-density units and high-density units is in the range of 31 mGal to 78 mGal values (Figure 6). If this value range is taken into account as a template, there are no remarkable changes in the values representing low and high-density units in the downward continuation maps representing depths of -1000 and -2000 meters from sea level. However, in the downward continuation map created for a depth of -3000 m, there is a significant change in values; at these depths, basic units are entered in places, and anomalies respond to inversion, reflections with deviations in the high and low-value ranges, and the values representing this response between low-density units and high-density units are between 208 mGal and -94 mGal (Figure 6). At -4000 m depths from the sea level, the noises reach the maximum size, the template value range disappears completely, and base units are entered in the whole area. In response, these values appear to be between 12185 mGal and -12097 mGal, which is unlikely to be on Earth or on similar planets.

Findings obtained with downward continuation maps reveal that density changes are not observed in units of about -4000 meters from sea level; in other words, base rocks are reached at these depths. Considering approximately 1000 m topography, it means talking about 5000 m depth from the surface.

The power spectrum graph consists of two different graphs as the total power-wave number and depth-wave number (Figure 7). It contains three

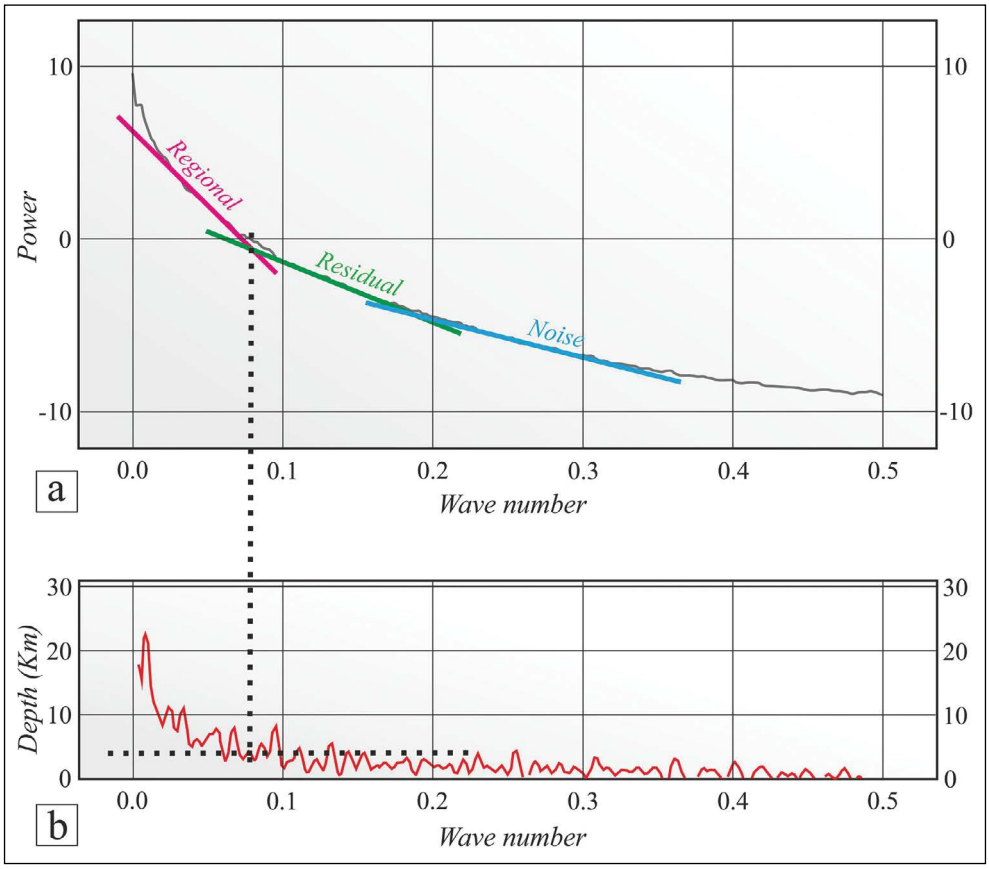

Figure 7- Graphs showing a) the average power spectrum and b) estimated depth obtained from isostatic gravity data.

lines with different inclined, which refers to the high power-wave number, the low power-wave number, and the very low power-wave number, respectively (Figure 7a). While the highly inclined line represents deep structures (regional), the line with low inclined indicates shallow structures (residual); the line with very low inclined corresponds to the undesired signals, which are called noise. By evaluating with the depth-wave graph and the power-wave number graph together allow us to determine the approximate depths of the basement rocks in the region and checking the values obtained from the estimation graph. The shallow and deep impact separation from the graph was determined as -4000 m to -5000 m depth. This depth is also consistent with the amount of depth obtained from the regional estimation graph.

4.3. Faults Obtained From Gravity Anomaly Values

Our gravity anomaly analysis in the area covering the TFZ and its surroundings indicate the presence of fault traces at levels of sea level (0 m) and -1000 m, -2000 m, -3000 m, and -4000 m depths (Figure 8). Fault traces limited by gravity anomaly analyzes in the region show mostly NW-SE orientation. Also,

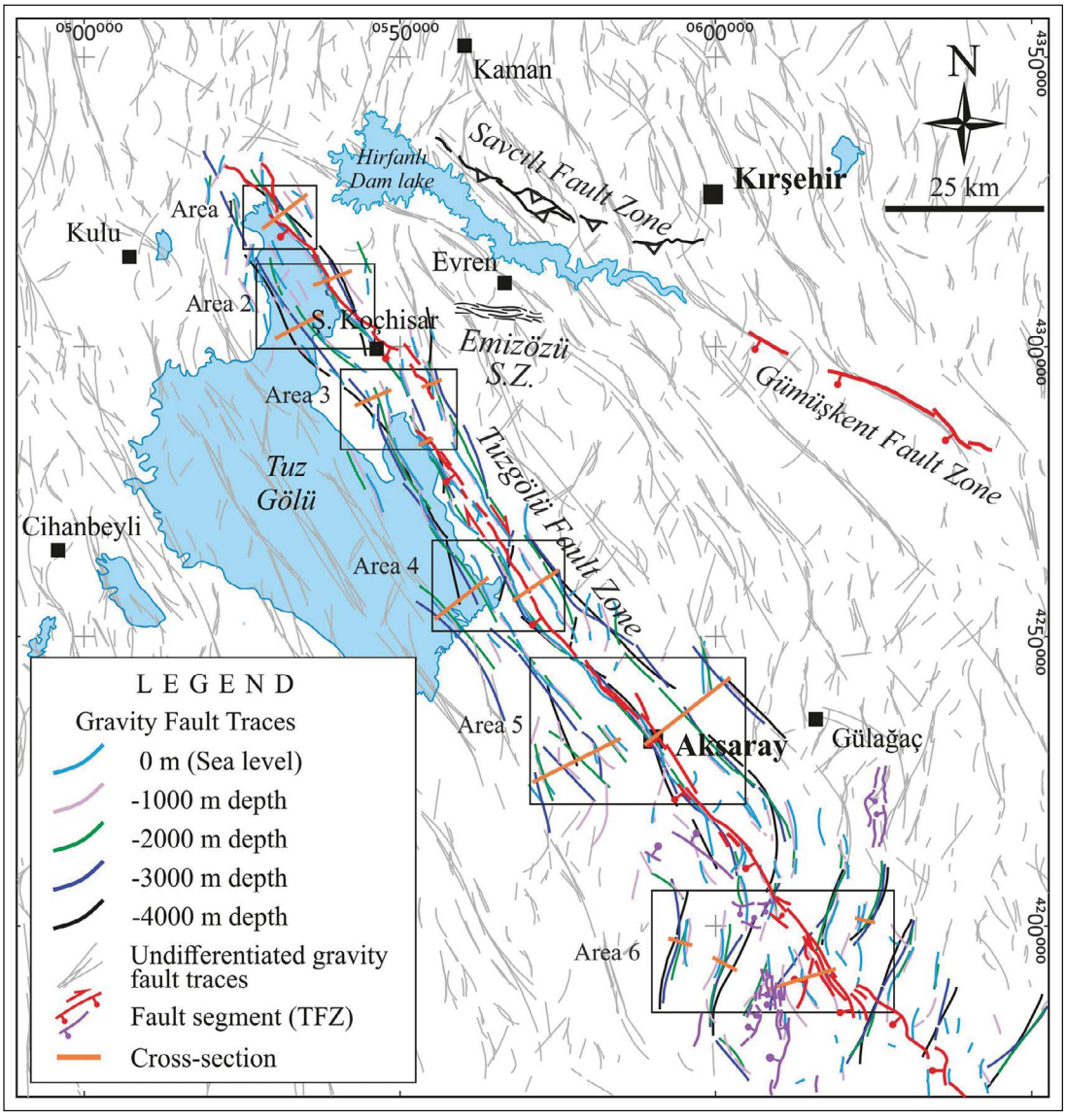

Figure 8- Map showing fault traces in-depth obtained from gravity anomalies along the TFZ and its surroundings. Fault strands of the Tuzgölü Fault Zone have adopted from MTA Active Fault Maps of Turkey (Emre et al., 2011). The Savcılı Fault Zone adopted from Çağlayan, 2010 and Işık et al., 2014.

there are fault traces with NE-SW and E-W trendings (Figure 8).

Within the scope of the study, gravity anomalies in six areas were studied in detail to determine the extending of the faults toward depth and their characteristics along the TFZ. The fault traces determined from gravity anomalies in each area were drawn on a map of the digital elevation model (DEM). The fault traces in these maps made for six areas are shown in different colors so that one could distinguish which faults appear in which levels. According to this; it is shown that faults at a depth of -4000 m from the sea level are black, faults at a depth of -3000 m are dark blue, faults at a depth of -2000 m are green in color, faults at a depth of -1000 m are lilac in color, and faults at a depth of 0 m referring to sea level light blue.

Amplitude and wavelength changes in gravity and magnetic anomalies provide lithology and depth estimation, respectively. Maximum and minimum changes of gravity anomalies of faults provide to determine the types of faults (Lowrie, 2007). It could be only possible that the faults at depths are mainly qualified as normal, reverse, and vertical faults using a method (Telford et al., 1990). In vertical faults, the ratio of maximum and minimum anomaly values is equal to 1. Anomaly defining the normal fault differs significantly from the anomaly of the vertical fault, and the ratio between the maximum and minimum anomaly values is less than 1. Similarly, the difference between these anomalies indicates the reverse faults, in which the ratio between the maximum and minimum anomaly values is greater than 1 (Telford et al., 1990). The type of all these faults is displayed using the appropriate symbol in the fault maps.

In order to better visualize the faults in the areas, the cross-sections were made up of every map. The type of faults is also marked on cross-sections considering their depths. In addition, the rose diagrams showing the orientation of fault traces in map areas were developed in case of understanding the main fault orientations at any level.

4.3.1. Area 1

Area 1 is located in the northwest extension of the TFZ. The TFZ is characterized by various structural segments (fault strands). The segments are commonly NW-SE-oriented; some of them strike to approximately N-S (Figures 9a, 9c). The segments along this part of the zone have a right-lateral strike-slip fault with a normal component. The gravity anomaly data in the region suggest evidence the faults at any level starting from sea level and towards 4000 m in depth. The rose diagram analysis indicates that the fault traces have NW-SE orientation, although the angle of strikes shows differences (Figures 9a, 9c). A lesser amount of these fault traces has an NNE-SSW orientation (Figure 9c). The type of most of these faults in area 1 is a normal fault. A limited number of fault traces show reverse and vertical fault characteristics (Figures 9a, 9b).

4.3.2. Area 2

Within Area 2, the fault segments representing the TFZ have an NW-SE trending and curved geometry. The fault type of segments comprises normal component strike-slip faults (Figure 10a). The gravity anomaly data indicate that these faults are of normal, reverse, and vertical fault character (Figures 10A, 10b, 10c). The rose diagram data show that the faults at depths of -4000 m and -3000 m are mostly similar to orientations (Figure 10d). A similar correlation could be made for faults at depths of -2000 m and -1000 m. These faults display NW-SE directions (Figure 10d). Our anomaly data suggest that the faults at depths along the TFZ have a normal fault with southwest dipping. While most of the faults occurred within the Tuz Gölü area and in the southwestern part of the map area are normal faults with northeast dipping, some of these faults show reverse fault character (Figures 10a, 10c). The fault traces identified at depths of -1000 m and sea level (0 m) are reverse faults. Both dip direction and hanging-wall and footwall relations suggest that sense of movement of the reverse faults is from the southwest to the northeast.

4.3.3. Area 3

The TFZ with fault segments in Area 3 step over to the northeast, and have an NW-SE trending with curved geometry (Figure 11a). The fault type of these segments is strike-slip faults with a normal component. The faults deduced from the gravity anomaly data in the area are mostly normal faults; a lesser amount of these faults display reverse fault characters (Figures 11a, 11b, 11c, 11d).

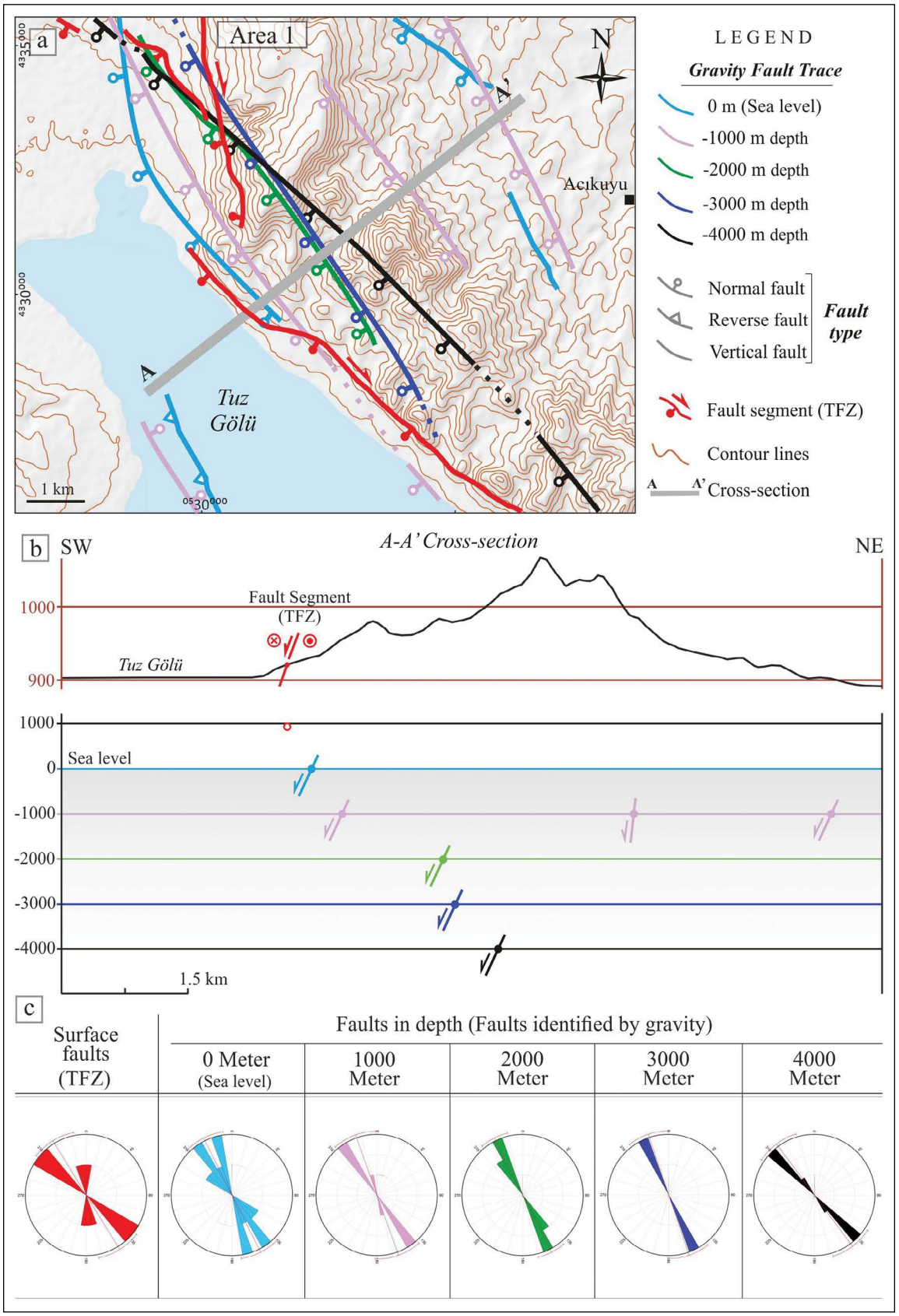

Figure 9- a) Map, b) cross-section and c) rose diagram view of the TFZ segments and fault traces in-depth obtained from gravity anomalies in Area 1.

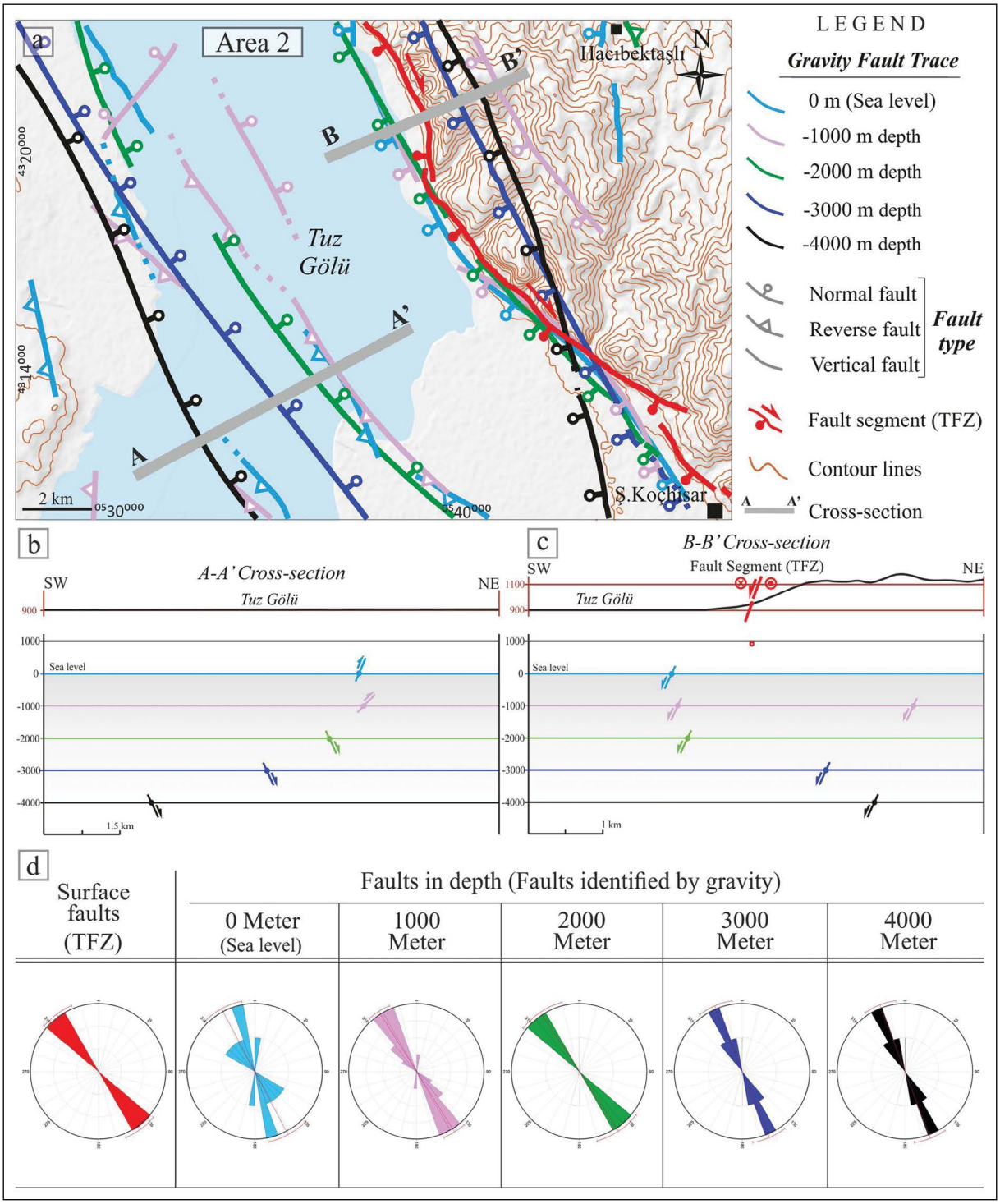

Figure 10- a) Map, b-c) cross-section and d) rose diagram view of the TFZ segments and fault traces in-depth obtained from gravity anomalies in Area 2.

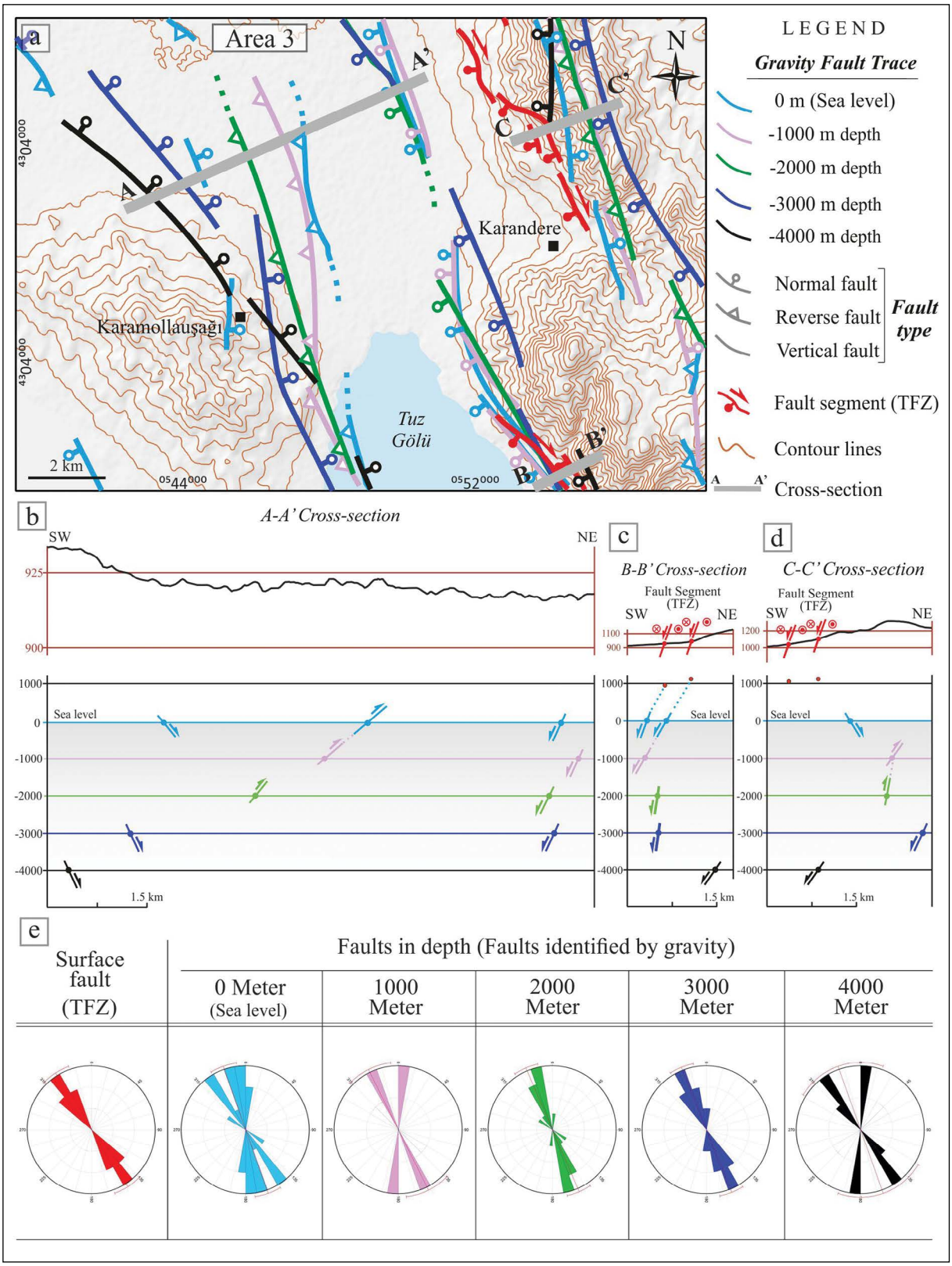

Figure 11- a) Map, b-c-d) cross-section and e) rose diagram view of the TFZ segments and fault traces in-depth obtained from gravity anomalies in Area 3.

Fault traces at depths of -4000 and -3000 m are normal fault characteristics; ₌2000 m, -1000 m, and some sea level faults have normal fault character, also (Figure 11b, 11c, 11d). The normal faults in an area dip to SW or NE. Some of the fault traces at -2000 m, and -1000 m depth is the reverse fault character. Dip directions and hanging-wall and footwall relations indicate that the reverse faulting originated in a movement from the southwest toward the northeast. The rose diagram data of the faults covering Area 3 reveal that the fault traces are mostly NW-SE trending; some of these fault traces have approximately N-S trending (Figure 11e).

4.3.4. Area 4

Area 4 covers an area located in the central part of the TFZ. The TFZ in this area includes a single fault segment. The segment strikes NW-SE and shows a strike-slip fault with a normal component. This active fault dip to the southwest (Figure 12a). The fault traces inferred from the gravity anomaly data is approximately NW-SE trending. Some of the faults at-4000 m depth have NNE-SSW striking (Figures 12a, 12d). These faults in Area 4 are of a normal and reverse faulting; some of these faults within a limited part of the areas are characterized by vertical faults. Fault traces at a depth of -4000 m are of a normal fault. Some of the faults at depths of -3000 and -2000 m and 0 m (sea level) are characterized by both a normal and reverse faulting (Figures 12a, 12b, 12c). Faults identified at depths of -1000 m in this area show reverse faulting with NE or SW dipping. The rose diagram pattern in Area 4 reveals that the fault traces are mainly in NW-SE orientation, but few fault traces have approximately N-W, NW-SSW, and NE-SW trends (Figure 12d).

4.3.5. Area 5

Area 5 is a region that includes the Aksaray settlement. The length of fault strands of the TFZ is between 4 km and 14 km in their lateral lengths. These faults have strike slip fault with a normal component. Fault traces inferred from gravity anomaly data form a typical fault zone geometry in the area. Most of the fault traces are NW-SE trending and dip to the southwest or northeast (Figure 13a). Most of these faults are characterized by a normal or reverse faulting. A limited number of faults have been identified as vertical faults (Figures 13b, 13c). As can be seen in the B-B' cross-section, the fault traces at -4000 m, -3000 m, and -2000 m depths are reverse faults with northeast dipping, unlike the fault strands of the TFZ. On the other hand, fault traces identified at -1000 m, and sea level depths are of a normal fault and are relatively compatible with the fault strands of the TFZ (Figures 13a, 13c). In the northeastern continuation of the same cross-section, the faults at-4000 m and -3000 m depths show normal faulting and dip to the southwest. Along the A-A' cross-section, The fault types in the Tuzgölü Basin differ. In this part, the fault traces at a depth of -2000 m are in reverse fault character. But the fault trace at a depth of -4000 m shows normal fault type. The faults identified at depths of -2000 m, -1000 m, and sea level along with the northeastern extension of the A-A' cross-section have noteworthy reverse faults feature (Figure 5b). The rose diagrams in Area 5 reveal that the fault traces are mostly in NW-SE trending (Figure 13d).

4.3.6. Area 6

Area 6 is located in the southeast extension of the TFZ. This part of the fault zone is characterized by dispersed geometry within a broad area. Due to such branching of fault strands suggest different fault orientations showing NW-SE, N-W, and NE-SW trending. In this area, the length of segments of the TFZ is between 1 km and 20 km in their lateral lengths. They show strike slip fault with a normal component (Figure 14a).

The orientation of the fault traces inferred from the magnetic anomaly data in the area is partially different from the other areas containing fault traces showing NNE-SSW and NE-SW orientation. The faults are mainly a normal or reverse faults. Some of these faults are also vertical fault (Figures 14a, 14b, 14c, 14d, 14e). Most of these faults have SE- or NW-dipping. All these orientations suggest that there might be relative rotation comparing the faults of the other areas. Most of the faults at a depth of -4000 m are in reverse fault character. Similar fault types are seen at depths of -3000 m and -2000 m. In this area, the fault traces inferred from the gravity data differ significantly with the fault segments of the TFZ (Figure 14). This difference is also seen in the rose diagrams for Area 6 (Figure 14f).

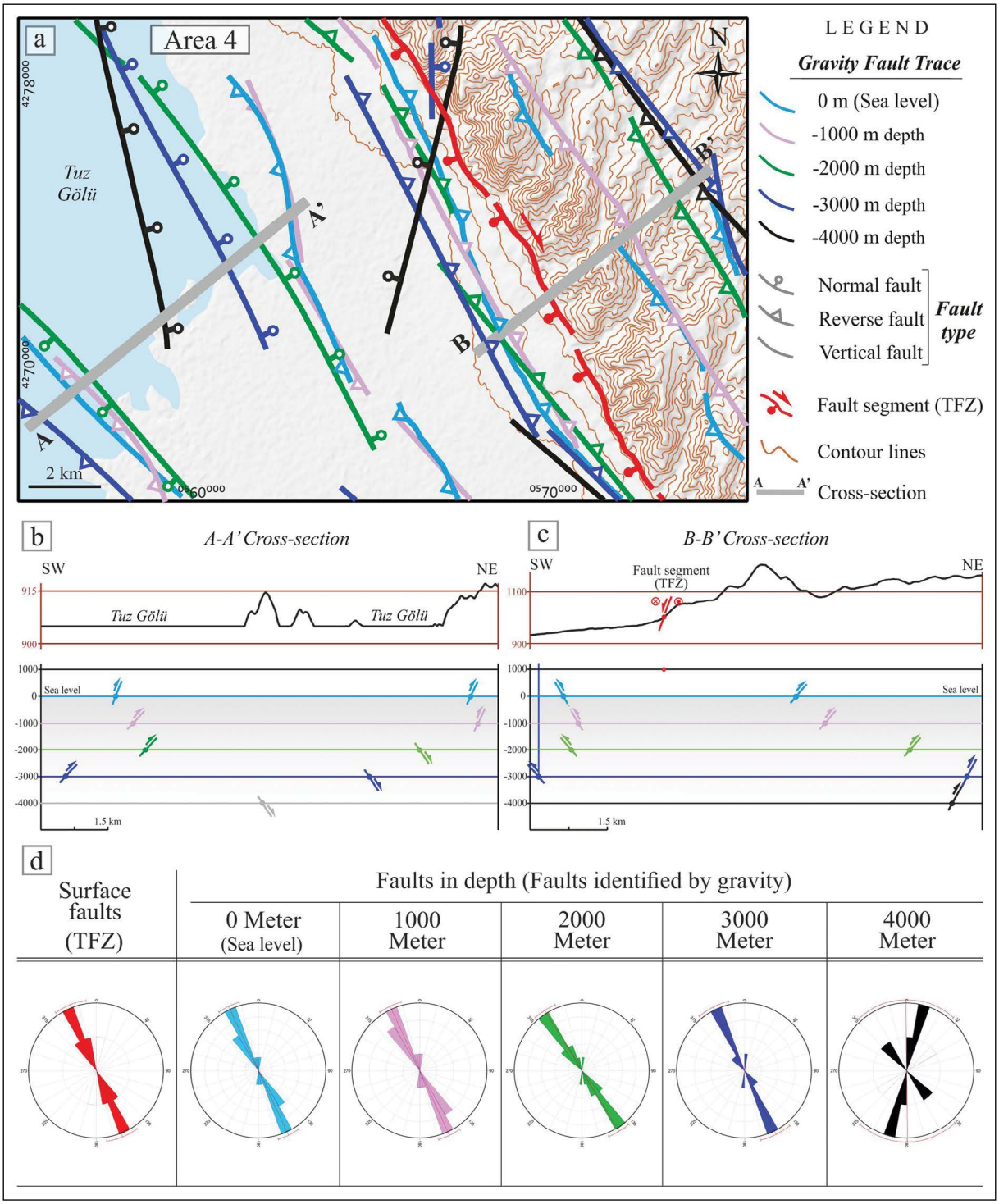

Figure 12- a) Map, b-c) cross-section and d) rose diagram view of the TFZ segments and fault traces in-depth obtained from gravity anomalies in Area 4.

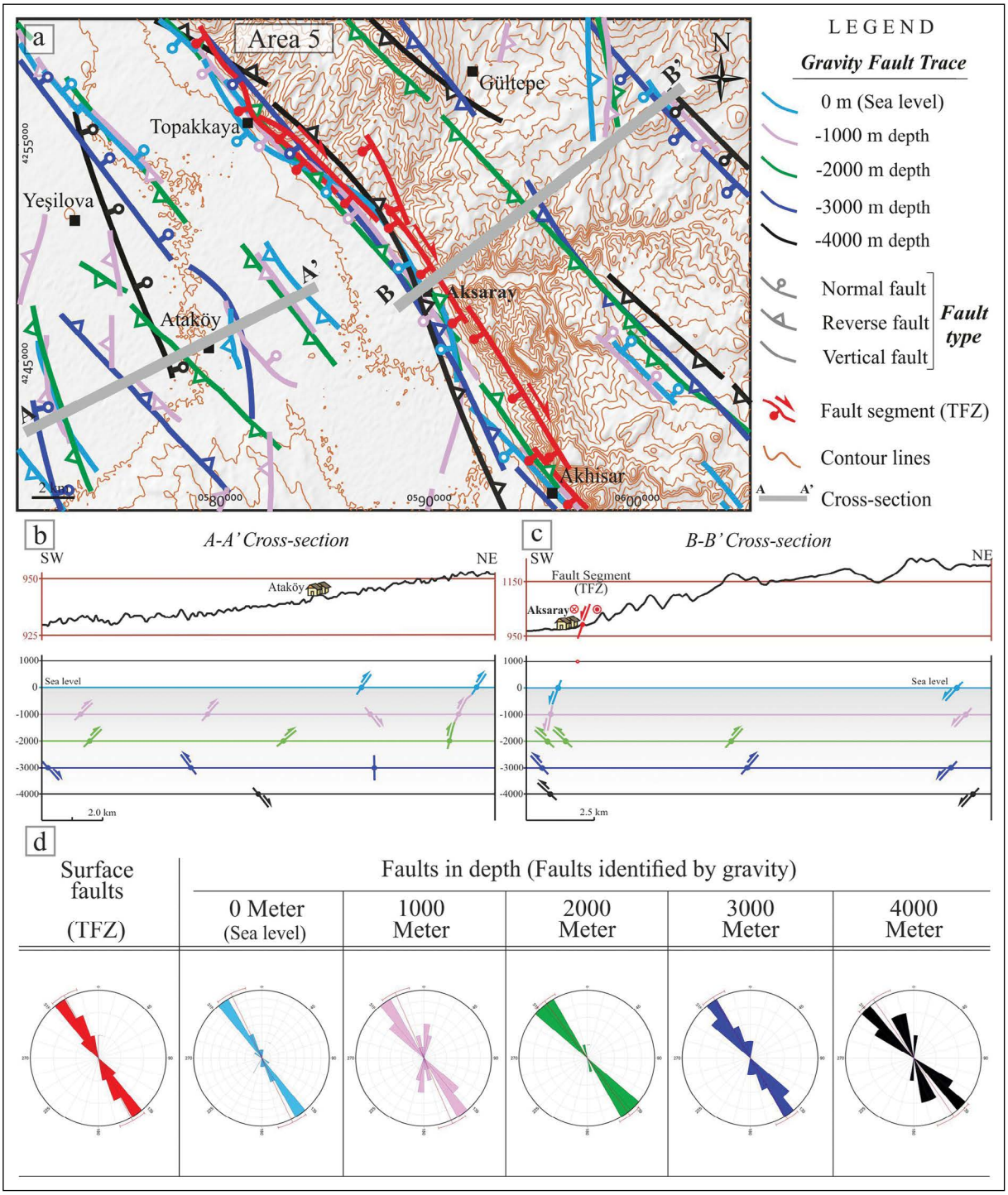

Figure 13- a) Map, b-c) cross-section and d) rose diagram view of the TFZ segments and fault traces in-depth obtained from gravity anomalies in Area 5.

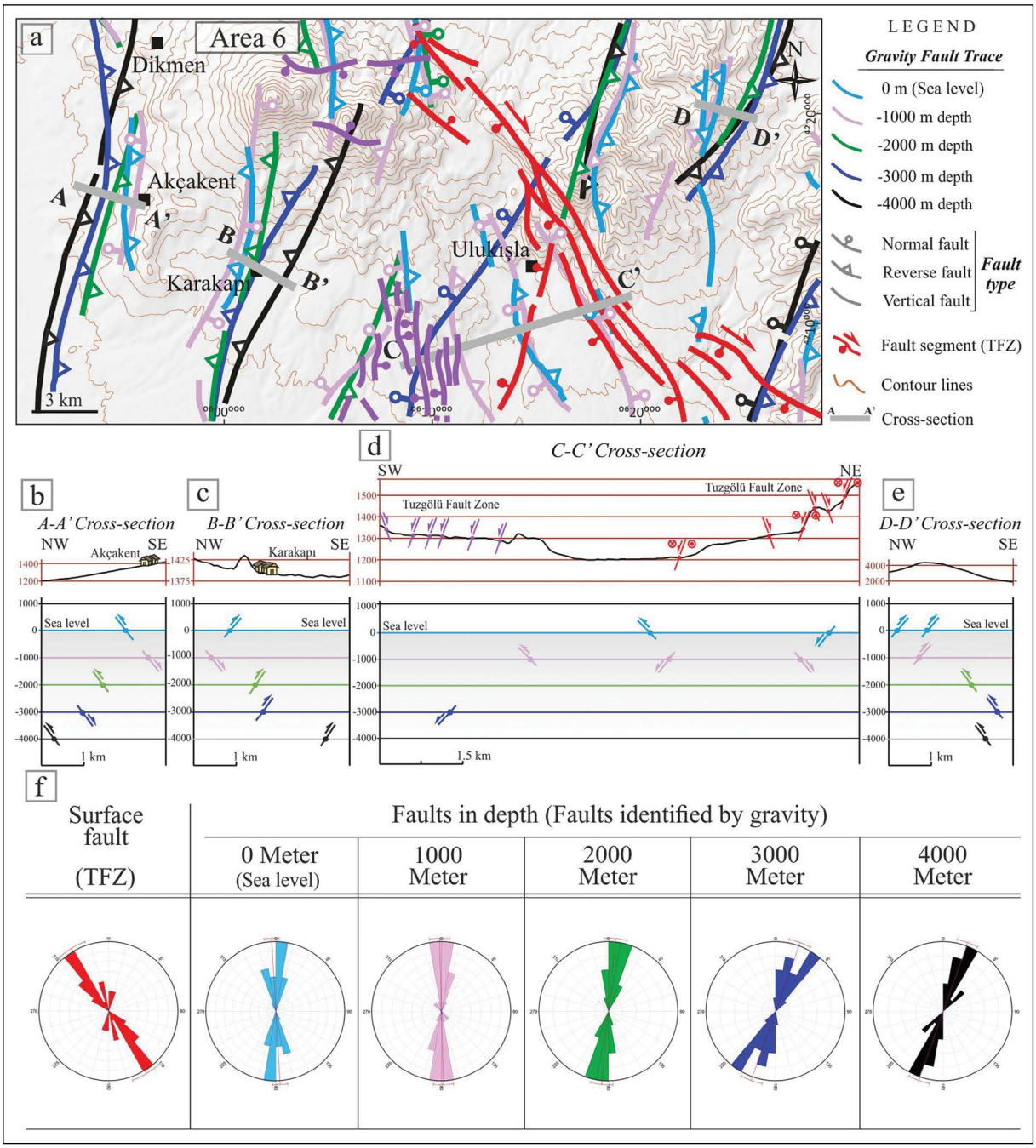

Figure 14- a) Map, b-c-d-e) cross-section and f) rose diagram view of the TFZ segments and fault traces in-depth obtained from gravity anomalies in Area 6.

5. Discussion

Central Anatolia includes many basin developments during the paleotectonic and neotectonic periods. These basins display a complex evaluation of the Neotethys Ocean in the late Cretaceous-Cenozoic period. Although it seems that these basins are different basins from each other based on recent positions in the region, it is known that some of them have the same or mutual geodynamic developments.

Geological-based detail studies state that units of the Central Anatolian Basins overlie both rocks of oceanic crust that represent the Neo-Tethyan Ocean and some rocks of continental crust (e.g., Sakarya Zone, Kırşehir Block) lithologies (Şengör and

Yılmaz, 1981; Görür et al., 1984; 1998; Koçyiğit et al., 1988; Koçyiğit, 1991; Göncüoğlu et al., 1996; Rojay, 2013). According to Görür et al. (1998), most of these basins are either arc-related or molasse basins. However, different evaluation mechanisms are suggested to these basins. (Çemen et al., 1999; Gürer and Aldanmaz, 2002; Derman et al., 2003; Alpaslan et al., 2006; Işık et al., 2008; 2014; Işık, 2009; Lefebvre et al., 2011; Advokaat et al., 2014; Seyitoğlu et al., 2017).

Tuzgölü Basin is one of the important basins in central Anatolia, which has kilometers of sediment thickness with broad distribution. The thickness of the basin deposits is estimated to be 9 km in the light of geological evidence (Görür et al., 1998). It is also interpreted based on geophysical methods (seismic, gravity, magnetic) that the average depth of the Tuzgölü Basin is 8 km, and even its some parts reach 12-13 km depth (Aydemir and Ateş, 2006*b*). Such thicknesses of deposits prove explicitly that the Tuzgölü Basin developed under fault control.

According to Görür et al. (1998), the Tuzgölü Basin is subduction-related arc basin with NE-SW trending that formed on the western side of boomerang-shaped Kırşehir Block and in the İzmir-Ankara Ocean. The researchers agree that the Tuzgölü Basin should be associated initially with the Çankırı, Kırıkkale and Ulukışla Basins and developed in same geodynamic conditions. Nairn et al. (2013) have been positioned the Tuzgölü Basin in the west of the Niğde-Kırşehir microcontinent in the Upper Cretaceous period, and they agree that the basin is associated with west-dipping subduction in the Neotethys Ocean. Yet these researchers, agree that the position of the Çankırı and Ulukışla Basins are different from that it is positioned by Görür et al. (1998). Çemen et al. (1999), Derman et al. (2003) and Dirik and Erol (2003) state that the Tuzgölü Basin continues in the Late Cretaceous-Early Paleocene stretched basin formation and continued in the Paleocene-Middle Eocene, and in the Late Eocene-Oligocene, the basin was affected by the compression regime, and during the Oligo-Miocene period basin also affected by the compressional regime. In Miocene-Early Pliocene, it represents basin development dominated by normal faulting.

Işık (2009) have mapped an extensional ductile shear zone to the northeast of the Tuzgölü Basin, Emizözü Shear Zone, which is responsible for the initiation of the Tuzgölü Basin. He pointed out that active TFZ should not be defined as the fault controlling the sedimentation of the Tuzgölü Basin since Cretaceous, and that the segments of the TFZ most probably occurred after Miocene. The age data from the faults forming the Savcılı Fault Zone using isotopic methods (Işık et al., 2014) present a significant contribution to the understanding of the geodynamic evaluation of the region. According to Işık et al. (2014), the Tuzgölü Basin started to form in Maastrichtian with the extensional regime accompanied by a ductile shear zone. The extensional regime has been replaced by the compression regime, represented by reverse faulting, from the middle Eocene (~ 46-40 Ma). The occurrence of these faults characterized by reverse faults continued until the Late Oligocene-Early Miocene (~ 30-23).

Seyitoğlu et al. (2017) have put forward the development of the basins in central Anatolia, especially the Ulukışla Basin, with the detachment fault in a regional model.

Fernandez-Blanco et al. (2013) suggest two independent basin development phases based on three-dimensional modeling with the help of some seismic reflection profiles for the Tuzgölü Basin. The first one is the Cenozoyic phase, and the other is the Late Miocene-Recent period phases. According to the researchers, the Cenozoyic phase represents the subduction of oceanic crust of the Sakarya Continent beneath the Kırşehir Massif, and thickening of the crust. These comments while supporting the view proposed by Görür et al. (1984); do not match the opinions suggested by Işık et al., 2008; 2014; Işık (2009) and Lefebre et al. (2011). According to Fernandez-Blanco et al. (2013), regional compression continued until the Late Miocene-Pliocene period. Then the extensional regime initiated in Tortonian and continued until recently, which is characterized by approximately 800 meters sediment deposition. However, the researchers also stated that the Late Miocene-Pliocene period could not be associated entirely with the extensional regime, but the basin might be affected by the main compression event for a short period (at the latest Miocene-Pliocene: 7-5 My). In the same study, the insufficiency of the evidence of this short-term compression regime in the Tuzgölü Basin is explained because of the extensional regime that obscures these structures. Unlike Fernandez-Blanco et al. (2013),

Özsayın et al. (2013), copartner of the same project, suggest a slightly different tectonic evaluation of the Tuzgölü Basin. In regard to Özsayın et al. (2013), the Tuzgölü Basin evaluated under two different tectonic regimes, which is before and after the upper Miocene. Accordingly, the compression regime in the basin, constrained by the Ar-Ar aging method (6.81 ± 0.24 Ma), continues until the upper Miocene, and then the basin is under the influence of the N-S and NE-SW extensional tectonic regime.

Understanding the faulting that occurred in the region helps the clarifying the tectonic evaluation of the region, where different views are asserted. The TFZ, the subject of this study, is one of the significant structural discontinuity because of its origin relationship with the Tuzgölü Basin mentioned (Figure 2). The surface geology studies show that the TFZ is an active fault zone with a length of approximately 195 km and a width between 1 km and 25 km. The zone is set mostly as Holocene faults in the Active Fault Map of Turkey produced by MTA 2011; some of these faults located in the southeastern part of the zone are also drawn as Quaternary faults. The majority of these faults in this map are characterized by normal faults and a lesser amount of them in local areas as strike-slip faults with normal components. Koçyiğit (2003) argues that TFZ is a dextral fault zone with normal components. Kürçer (2012) and Kürçer and Gökten (2014) suggest that the zone consists of different segments represented by oblique faulting with normal components.

Due to the possible oil potential of the Tuzgölü Basin, deep drilling and seismic profile studies were carried out in different parts of the basin. Numerous seismic profile sections in the basin covering the TFZ were extrapolated and suggested various structure occurrences for the region.

Uğurtaş (1975) propounded that the subsurface of the Tuz Gölü area includes salt structures based on seismic reflection profiles, gravity, and surface topography data. Çemen et al. (1999) point out based on the interpretation of the seismic profile perpendicular to the TFZ in the northwest of Aksaray that the basin is bordered by, a normal fault with high-angle in the near-surface of the Tuzgölü Basin and, by a low-angle detachment fault, its downward continuation and the basin deposits display folding with anticline geometry to this fault. Similar seismic profiles of the Tuzgölü Basin were also used by Aydemir and Ateş (2006*b*), and their seismic profile interpretations suggest the development of normal faultings with different displacements. Examination of these seismic profiles has also been subjected to the study of Fernandez-Blanco et al. (2013). From the seismic profiles with a depth of approximately 7 km and traverse the TFZ, the evidence of the normal fault with extending kilometers toward depth is interpreted, which is called Tuzgölü Fault. The interpretation of the profile sections in the same study, the presence of the post-Pliocene thrust fault (Şereflikoçhisar-Aksaray Thrust) which extends to the depths in the hanging wall is also remarked.

Işık (2009) records ductile (mylonitic) shear zone (Emizözü Shear Zone) with N70°-80°W trending and southwest dipping that cut the Ağaçören Granitoid in the Central Anatolian Crystalline Complex between Evren and Şereflikoçhisar (Figure 2). The microstructural features of the Emizözü Shear Zone reveal that the zone has occurred with the regional extensional regime; the age of the zone is reported as 78-71 Ma (Işık, 2009). Lefebvre et al. (2011) define the detachment zone, 84-74 Ma age, in the vicinity of Kaman, which advocates the Late Cretaceous extensional tectonic regime proposed by Işık (2009). Another similar extensional ductile shear zone was described in the northern part of the Central Anatolian Crystalline Complex (Işık et al., 2008). Seyitoğlu et al. (2017) present a geological model for the extensional regime of the region covering all these ductile shear zones and the Ivriz Detachment Fault that is responsible for controlling part of deposits in the Ulukışla Basin located in the southern part of Central Anatolia.

Işık et al. (2014) indicate the following tectonic development based on field findings and observations and isotopic age data for Central Anatolia: Central Anatolia is exposed to the extensional regime in the latest Cretaceous during the closure of the Neo-Tethyan Ocean associated with the regional compressional regime. The extensional regime in Central Anatolia is characterized by the emplacement of granitoid intrusion, the development of ductile shear zones, the rising and exhumation of metamorphites and granitoids, and the opening of major basins associated with normal faultings. Then, from the Middle Eocene, the extensional regime gave way to the compressional regime, which causes the development of reverse and

thrust faults in the region commonly. The Savcılı Fault Zone, well-known its age of faulting, is the typical example of the compressional regime. Isotopic age data indicate that this compressional regime lasted until the end of Oligocene or earliest Miocene (Işık et al., 2014). The next period is explicated either extensional or lateral tectonic regime or both. Geological cross-sections in the Tuzgölü Basin set by Dellaloğlu and Aksu (1984) also have the reverse and thrust faults developed in the pre-Miocene period. Borehole data obtained from drilling for hydrocarbon exploration verified the existence of these faults. Remarkably, some of these faults that present in the depth of the basin have similar tectonic movement of the Savcılı Fault Zone. However, there are different views and interpretations about Savcılı Fault Zone (Yürür and Genç, 2006; Lefebvre et al., 2013; Gürer and van Hinsbergen, 2019).

Palaeomagnetic studies have been carried out for a better understanding of structural discontinuities and the spatial and temporal development of lithology in the geology of Turkey. In this context, sense and amount of rotation in local and regional areas have been estimated by using paleomagnetic data obtained from lithologies formed in different ages (Tatar et al., 1996; Gürsoy et al., 1997; 1998; Platzman et al., 1998; Kaymakçı et al., 2003; Kissel et al., 2003; Lefebvre et al., 2013; Çinku et al., 2016; Gürer et al., 2018). Interpretation of the paleomagnetic data obtained from Central Anatolia would be different. Differences in interpretations can vary depending on the type of lithology, the number of samples, and the quality of data. According to Platzman et al. (1998), Central Anatolia has shown a 50° counterclockwise rotation from 12 Ma until recently. Kissel et al. (2003) suggest that Kırşehir Block might be rotated ~ 25° counterclockwise in the Neogene period.

Recently, paleomagnetic measurements performed by Çinku et al. (2016) Mesozoic and Cenozoic units of the Kırşehir Block and Central Taurides show that Central Anatolia record quite complex rotational movements. Accordingly, the upper Cretaceous ophiolitic rocks in west of Kırıkkale and southwest of Yozgat have a clockwise rotation of 26.2° and counterclockwise rotation of 15.5°, respectively. In the same study, counterclockwise rotations of 39.5°±9.9° and 51.5°±13.1° have been estimated in the Tuzgölü Basin, where the place in the northwest extension of the TFZ, and the Ulukışla Basin located in the south-southwest part of the zone and Tuzgölü Basin, respectively. The counterclockwise rotation of 85.5°±19.3° have been suggested in the Tuz Gölü area for the Middle Eocene (Çinku et al., 2016). Also, rotations, mostly counterclockwise and clockwise, have been recorded in widely distributed Niğde and Kırşehir massive areas containing units of the Late Cretaceous-Middle Eocene, Late Cretaceous-Paleocene and Middle Eocene. The range of rotation amounts in the massive areas is distinctly high (Çinku et al., 2016). The researchers have explained that different sense and amount of rotations of paleomagnetic data obtained from regions in Central Anatolia result from the regional faultings. (Lefebvre et al., 2013; Lucifora et al., 2013; Çinku et al., 2016; Gürer et al., 2018). Fault traces (from sea level to -4000 m depth) obtained from the analysis of gravity and magnetic measurements have mainly NW-SE orientation. The initial position of these faults at depth along the TFZ were most probably NNW-SSE and/or N-S orientation if it is considered that Central Anatolia experienced counterclockwise rotations between 25° and 50° for the Neogene (Platzman et al., 1998; Kissel et al., 2003),

6. Conclusions

In this study, we have identified faulting mechanisms in TFZ and its surroundings based on the analysis of gravity and magnetic measurements. Obtained data suggest the following results:

(1) The faults located at sea level (0 m), -1000 m, -2000 m, -3000 m, and -4000 m depths along the Tuzgölü Fault Zone and in its surroundings were determined using the gravity anomaly data.

(2) The lateral extent of the fault traces in these depths ranges from a few kilometers to several tens of kilometers. This NW-SE, N-S, and NE-SW oriented faults show mostly normal and reverse fault characteristics and few numbers of vertical faults. Considering rotational amounts specified for the Paleogene period based on paleomagnetic data in Central Anatolia, it appears that these faults will have slightly different orientations from their present location, many of which are probably represented by NNW-SSE and N-S directions.

(3) Area 1 and Area 2, located in the northwestern extension of Tuzgölü Fault Zone, are mostly dominated by normal faulting. These faults at sea level (0 m), -1000 m, -2000 m, -3000 m and -4000 m depths are dipping to the NE and SW according to the fault trace, and control the sedimentation processes in the Tuzgölü Basin.

(4) Some of the faults identified in depths, from Şereflikoçhisar to the southeastern extension of the Tuzgölü Fault Zone (Area 3, Area 4, Area 5 and Area 6), exhibit reverse fault characteristics. In particular, reverse faults are noteworthy in areas close to the fault strands of active Tuzgölü Fault Zone in Area 4 and Area 5. Compared to other regions, the faults determined along Area 6 are mostly NE-SW oriented.

(5) In the studied areas, among the faults determined from sea level up to -4000 m, those with normal fault characteristics were interpreted as faults controlling the development of the Tuzgölü Basin and the deposition of the basin sediments. The reverse faults, which can be correlated with the faulting ages obtained by Işık et al. (2014) (Middle Eocene: ~ 46-40 My and Late Oligocene-Early Miocene: ~ 30-23), were interpreted as a result of the compression regime that occurred during this period.

(6) The faulting characteristics along the zone reveals that Tuzgölü Basin has not been under the same tectonic regime from the Late Cretaceous to the present day. Moreover, our findings contradict some literature data about the geology of the region, suggesting that the eastern part of the Tuzgölü basin has limited by a single fault trace and that this trace is associated with a single normal fault that continues to depth for kilometers. In particular, reverse faulting revealed in this study, contracts with previous studies based on the seismic profiles in the region, which only highlight the role of normal faulting in the evolution of the basin. It contracts with the faulting models which propose high angle normal faults near the surface that their dips decrease in depths, also. These indicate that seismic profile interpretations should be reviewed. Some of the reverse faulting presented in this study seems to be compatible with the Şereflikoçhisar-Aksaray Thrust revealed by Fernandez-Blanco et al. (2013).

(7) The normal faults identified along the Tuzgölü Fault Zone and its nearby surroundings mainly represent the Late Cretaceous-Middle Eocene and early Miocene-Quaternary periods. The reverse faults also represent the Middle Eocene-Late Oligocene / Early Miocene time interval. The fault segments representing the Tuzgölü Fault Zone and indicated on the MTA Active Fault Map are relatively younger structures in comparison to these faults, which should be formed after Middle Miocene or Early Pliocene.

Acknowledgements

Dr. Ayşe Çağlayan and Reza Saber are thanked for scientific discussion, useful suggestions, and their substantial advice during manuscript preparation. The authors also sincerely thank Prof. Dr. Bora Rojay, Sait Yüksel, Prof. Dr. Nurettin Kaymakçı, and the anonymous reviewers for their constructive and critical comments on an earlier version of this manuscript.

References

Advokaat, E.L., Van Hinsbergen, D.J.J., Kaymakçı, N., Vissers, R.L.M., Hendriks, B.W.H. 2014. Late Cretaceous extension and Palaeogene rotation-related contraction in Central Anatolia recorded in the Ayhan-Büyükkışla basin. International Geology Review 56, 1813-1836.

Alpaslan, M., Boztuğ, D., Frei, R., Temel, A., Kurt, M.A. 2006. Geochemical and Pb-Sr-Nd isotopic composition of the ultrapotassic volcanic rocks from the extension - related Çamardı-Ulukışla basin, Niğde province, central Anatolia, Turkey. Journal of Asian Earth Sciences 27, 613-627.

Arıkan, Y. 1975. The Geology and Petroleum Prospects of The Tuz Gölü Basin. Bulletin of the Mineral Research and Exploration 85, 17-37.

Ateş, A. 1999. Possibility of deep gabbroic rocks, east of Tuz Lake, central Turkey, interpreted from aeromagnetic data. Journal of the Balkan Geophysical Society 2(1), 15-29.

Aydar, E., Gourgaud, A. 2002. Garnet-bearing basalts: an example from Mt. Hasan, Central Anatolia, Turkey. Mineralogy and Petrology 75, 185-201.

Aydar, E., Gündoğdu, M., Bayhan, H., Gourgaud, A. 1994. Kapadokya bölgesi, Kuvaterner yaşlı volkanizmasının volkanik-yapısal ve petrolojik incelemesi. Doğa - Yerbilimleri 3, 25-42.

Aydemir, A., Ateş, A. 2006*a*. Interpretation of Suluklu-Cihanbeyli- Goloren Magnetic Anomaly, Central Anatolia, Turkey: An integration of geophysical data. Physics of the Earth and Planetary Interiors 159, 167-182.

Aydemir, A., Ateş, A. 2006*b*. Structural interpretation of the Tuzgolu and Haymana Basins, Central Anatolia, Turkey, using seismic, gravity and aeromagnetic data. Earth Planets Space 58, 951-961.

Aydemir , A., Ateş, A. 2008. Determination of hydrocarbon prospective areas in the Tuzgolu (Saltlake) Basin, Central Anatolia, by using geophysical data Journal of Petroleum Science and Engineering 62, 36-44.

Aydın, A. 1997. Gravite verilerinin Normalize Edilmiş Tam Gradyan,Varyasyon ve İstatistik ile Hidrokarbon Açısından Değerlendirilmesi, Model Çalışmalar ve Hasankale-Horasan (Erzurum) Havzasının Uygulanması. Doktora Tezi, Karadeniz Teknik Üniversitesi, 151s. Trabzon (unpublished).

Aydoğan, D. 2011. Extraction of lineaments from gravity anomaly maps using the gradient calculation: Application to Central Anatolia. Earth Planets and Space 63(8), 903-913.

Baldwin, R., Langel, R. 1993. Tables and Maps of the DGRF 1985 and IGRF 1990. International Union of Geodesy and Geophysics Association of Geomagnetism and Aeronomy (IAGA Bulletin) 54, 158s.

Beekman, P. 1966. The Pliocene and Quaternary volcanism in the Hasan Dag- Melendiz Dag region. Bulletin of the Mineral Research and Exploration 66, 90-105.

Besang, C., Eckhart, F., Harre, W., Kreuzer, H., Müller, P. 1977. Radiometrische altersbestimmungen an neogenen eruptigesteinen der Tukei. Geol. Jahrb. B25, 3-36.Blakely, R. 1995. Potential Theory In Gravity and Magnetic Applications. Cambridge University Press 441 p.

Blakely, R. 1995. Potential Theory In Gravity and Magnetic Applications. Cambridge University Press, 441 p.

Blakely, R., Simpson, R. 1986. Approximating edges of source bodies from magnetic or gravity anomalies. Geophysics 51(7), 1494-1498.

Boschetti, F. 2005. Improved edge detection and noise removal in gravity maps via the use of gravity gradients. Journal of Applied Geophysics 7(3) 213-225.

Cooper, G., Cowan, D. 2008. Edge enhancement of potential-field data using normalized statistics. Geophysics 73(3), 1MJ-Z46.

Cordell, L. 1979. Gravimetric Expression of Graben Faulting In Santa Fe Contry and The Espanola Basin, New Mexico. In: Ingersoll, R.V., Woodward, L.A., James, H.L. (Ed.), New Mexico Geological Society 30 th Annual Fall Field Conference Guidebook to Santa Fe Country, Socorro 59-64.

Cordell, L.E., Grauch, V.J.S. 1982. Reconciliation of the discrete and integral Fourier transform. Geophysics, 47, 237-243.

Cordell, L.E., Grauch, V.J.S. 1985. Mapping basement magnetization zones from aeromagnetic data in the San Juan Basin, New Mexico. In The utility of regional and magnetic anomaly maps. Edited W.J. Hinze. Society of Exploration Geophysicists 181-197.

Çağlayan, A. 2010. Savcılı Fay Zonunun Yapısal Analizi. Yüksek Lisans Tezi, Ankara Üniversitesi, 82s. Ankara (unpublished).

Çemen, İ., Göncüoğlu, M., Dirik, K. 1999. Structural evolution of the Tuzgölü basin in Central Anatolia Turkey. Journal of Geology 107(6), 693-706.

Çinku, M. C., Hisarli, Z. M., Yılmaz, Y., Ülker, B., Kaya, N., Öksüm, E., Orbay, N., Özbey, Z. Ü. 2016. The tectonic history of the Niğde-Kırşehir Massif and the Taurides since the Late Mesozoic: Paleomagnetic evidence for two-phase orogenic curvature in Central Anatolia. Tectonics 35, 772-811.

Dellaloğlu, A., Aksu, R. 1984. Kulu-Şereflikoçhisar-Aksaray dolayının jeolojisi ve petrol olanakları. TPAO Rapor No: 2020, Ankara (unpublished).

Deniel, C., Aydar, E., Gourgaud, A. 1998. The Hasan Dağı stratovolcano (Central Anatolia, Turkey): evolution from calc-alkaline to alkaline magmatism in a collision zone. Journal Volcanology And Geothermal Research 87, 275-302.

Derman, A., Rojay, B., Güney, H., Yıldız, M. 2003. Şereflikoçhisar-Aksaray fay zonu'nun evrimi hakkında yeni veriler. Türkiye Petrol Jeologları Derneği Özel sayı 5, 47-70.

Dirik, K., Göncüoğlu, M. 1996. Neotectonic characteristics of Central Anatolia. International Geology Review 38, 807-817.

Dirik, K., Erol, O. 2003. Tuzgölü ve çevresinin tektonomorfolojik evrimi, Orta Anadolu-Türkiye. Türkiye Petrol Jeologları Derneği Özel sayı 5, 27-46.

Emre Ö., Duman, T.Y., Özalp, S., Elmacı, H., Olgun, Ş. 2011. 1:250.000 ölçekli Türkiye Diri Fay Haritası Serisi, Aksaray (NJ 36-7) Paftası, Seri No: 26, Kırşehir (NJ 36-3) Paftası, Seri No: 25, Karaman (NJ 35-11) Paftası, Seri No: 27, Maden Tetkik ve Arama Genel Müdürlüğü, Ankara.

Ercan, T., Tokel, S., Matsuda, J., UI, T., Notsu, K., Fujitani, T. 1992. Hasandağı-Karacadağ (Orta Anadolu) Kuvaterner volkanizmasına ilişkin yeni jeokimyasal, izotopik ve radyometrik veriler. Türkiye Jeoloji Bülteni 7, 8-21.

Eren, Y. 2003*a*. Konya bölgesinin depremselliği. Türkiye Petrol Jeologları Derneği Özel sayı 5, 85-98.

Eren, Y. 2003*b*. Tuzgölü Havzası güneybastısındaki (Altınekin-Konya) temel kayaçlarının jeolo0jisi. Türkiye Petrol Jeologları Derneği Özel Sayı 5, 113-116.

Fernandez-Blanco, D., Bertotti, G., Çiner, A. 2013. Cenozoic tectonics of the Tuz Gölü Basin (Central Anatolian Plateau, Turkey). Turkish Journal of Earth Sciences 22, 715-738.

Göksu, B. 2015. Cihanbeyli-Yeniceoba (Konya Kuzeyi) Civarındaki Miyo-Pliyosen Birimlerin Sedimantolojisi. Yüksek Lisans Tezi, Ankara Üniversitesi, 188s. Ankara (unpublished).

Göncüoğlu, M.C., Erler, A., Toprak, V., Yalınız, K., Olgun, E., Rojay, B. 1992. Orta Anadolu Masifinin Batı Bölümünün Jeolojisi. Bölüm 2: Orta Kesim TPAO Rapor No: 3535, Ankara (unpublished).

Göncüoğlu, M., Türeli, T. 1993. Petrology and geodynamic interpretation of plagiogranites from central Anatolian ophiolites (Aksaray-Turkey). Turkish Journal of Earth Sciences 2, 195-203.

Göncüoğlu, M., Dirik, K., Erler, A., Yalınız, K., Özgül, L., Çemen, İ. 1996. Tuzgölü havzası batı kısmının temel jeolojik sorunları. TPAO Rapor No: 3753, Ankara (unpublished).

Görür, N., Oktay, F., Seymen, İ., Şengör, A. M. C. 1984. Paleotectonic evolution of the Tuzgölü Basin Complex, Central Turkey: Sedimentary record of a Neo-Tethyan closure, in Dixion, J.E. and Robertson A.H.F. eds., The Geological Evolution of the Eastern Mediterranean. Geological Society of London Special Publications 17, 455-466.

Görür, N., Tüysüz, O., Şengör, A.M.C. 1998. Tectonic evolution of the Central Anatolian basins. International Geology Review 40, 831-850.

Gülyüz, E., Kaymakçı, N., Meijers, M.J.M., Van Hinsbergen, D.J.J., Lefebvre, C., Vissers, R.L.M., Hendriks, B.W.H., Peynircioğlu, A.A. 2013. Late Eocene evolution of the Çiçekdağı Basin (central Turkey): syn-sedimentary compression during microcontinent - continent collision in central Anatolia. Tectonophysics 602, 286–299.

Gürbüz, A. 2012. Tuz Gölü Havzası'nın Pliyo-Kuvaterner'deki Tektono- sedimanter evrimi. Doktora Tezi, Ankara Üniversitesi, 130 s Ankara (unpublished).

Gürer, Ö.F., Aldanmaz, E. 2002. Origin of the Cretaceous-Tertiary sedimentary basins within the Tauride-Anatolide platform in Turkey. Geological Magazine 139, 191-197.

Gürer, D., van Hinsbergen, D.J.J. 2019. Diachronous demise of the Neotethys Ocean as a driver for non-cylindrical orogenesis in Anatolia. Tectonophysics 760, 191-211.

Gürer, D., van Hinsbergen, D.J.J., Özkaptan, M., Creton, I., Koymans, M.R., Cascella, A., Langereis, C.G. 2018. Paleomagnetic constraints on the timing and distribution of Cenozoic rotations in Central and Eastern Anatolia. Solid Earth 9, 295-322.

Gürsoy, H., Piper, J.D.A., Tatar, O., Temiz, H. 1997. A palaeomagnetic study of the Sivas Basin, Central Turkey: Crustal deformation during lateral escape of the Anatolian Block. Tectonophysics 271, 89-106.

Gürsoy, H., Piper, J.D.A., Tatar, O., Mesci, L. 1998. Paleomagnetic study of the Karaman and Karapinar volcanic complexes, central Turkey: Neotectonic rotation in the south-central sector of the Anatolian block. Tectonophysics 299, 191-211.

Hosseini, S., Ardejani, F., Tabatabaie, S., Hezarkhani, A. 2013. Edge Detection in Gravity Field of the Gheshm Sedimentary Basin. International Journal of Mining and Geo-Engineering Article 4 47(1), 41-50.

Huestis, S. P., Parker, R. L. 1979. Upward and Downward Continuation as Inverse Problems. Geophysical Journal of the Royal Astronomical Society 57, 171-188.

Işık, V., C., Göncüoğlu, C., Demirel, S. 2008. $^{39}Ar/^{40}Ar$ ages from the Yozgat Batholith: Preliminary data on the timing of Late Cretaceous extension in the Central Anatolian Crystalline Complex, Turkey. Journal of Geology 116(5), 510-526.

Işık, V. 2009. Ductile shear zone in granitoid of Central Anatolian Crystalline Complex, Turkey: Implications for Late Cretaceous extensional deformation. Journal of Asian Earth Science 34, 507-521.

Işık, V., Uysal, T., Çağlayan, A., Seyitoğlu, G. 2014. The evolution of intra-plate fault system in central Turkey: structural evidence and Ar-Ar and Rb-Sr age constrains for the savcılı Fault Zone. Tectonics 33(10), 1875-1899.

İlkışık, O., Gürer, A., Tokgöz, T., Kaya, C. 1997. Geoelectromagnetic and geothermic investigations in the Ihlara Valley geothermal field. Journal of Volcanology and Geothermal Research 78, 297-308.

Karaman, E. M. 1986. Altınekin (Konya) çevresinin jeolojik ve tektonik evrimi. Türkiye Jeoloji Bülteni 29(1), 157-171.

Kaymakçı, N., Duermeijer, C.E., Langereis, C.G., White, S.H., Van Dijk, P.M. 2003. Palaeomagnetic evolution of the Çankırı Basin (central Anatolia, Turkey): implications for oroclinal bending due to indentation. Geological Magazine 140 (3), 343-355.

Keskin, M., Genç, S.C., Tüysüz, O. 2008. Petrology and geochemistry of post-collisional Middle Eocene volcanic units in North-Central Turkey: evidence for magma generation by slab breakoff following the closure of the Northern Neotethys Ocean. Lithos 104, 267-305.

Ketin, İ. 1966. Tectonic Units of Anatolia (Asia Mınor). Bulletin of the Mineral Research and Exploration 66, 20-35.

Kissel, C., Laj, C., Poisson, A., Görür, N. 2003. Paleomagnetic Reconstruction of the Cenozoic Evolution of the Eastern Mediterranean. Tectonophysics 362, 199-217.

Koçyiğit, A. 1991. An example of an accretionary forarc basin from northern Central Anatolia and its implications for the history of subduction of Neo-Tethys in Turkey. Geological Society of America Bulletin 103, 22–36.

Koçyiğit, A. 2003. Orta Anadolu'nun genel neotektonik özellikleri ve depremselliği. Türkiye Petrol Jeologları Derneği Özel Sayı 5, 1-26.

Koçyiğit, A., Özkan, S., Rojay, B.F. 1988. Examples from the fore-arc basin remnants at the active margin of northern Neotethys; Development and emplacement age of the Anatolian Nappe, Turkey. METU Journal of Pure and Applied Sciences 21(1-3), 183-210.

Köksal, S., Romer, R.L., Göncüoğlu, M.C., Toksoy-Köksal, F. 2004. Timing of post-collision H-type to A-type granitic magmatism: U-Pb titanite ages from the Alpine central Anatolian granitoids Turkey. International Journal of Earth Sciences 93, 974-989.

Kürçer, A. 2012. Tuz Gölü Fay Zonu'nun Neotektonik Özellikleri ve Paleosismolojisi, Orta Anadolu, Türkiye. Doktora Tezi, Ankara Üniversitesi, 318 sayfa, Ankara (unpublished).

Kürçer, A., Gökten, Y. 2014. Neotectonic-Period Characteristics, Seismicity, Geometry And Segmentation Of The Tuz Gölü Fault Zone. Bulletin of the Mineral Research and Exploration 149, 19-69.

Lefebvre, C., Barnhoorn, A., Van Hinsbergen, D.J.J., Kaymakçı, N., Vissers, R.L.M. 2011. Late Cretaceous extensional denudation along a marble detachment fault zone in the Kırşehir massif near Kaman, central Turkey. Journal Structural Geology 33, 1220-1236.

Lefebvre, C., Meijers, M.J.M., Kaymakçı, N., Peynircioğlu, A., Langereis, C. G., Van Hinsbergen, D.J.J. 2013. Reconstructing the geometry of central Anatolia during the late Cretaceous: Large-scale Cenozoic rotations and deformation between the Pontides and Taurides. Earth and Planetary Science Letters 366, 83-98.

Lowrie, W. 2007. Fundamentals of Geophysics. Second Edition Published in the United States of America by Cambridge University Press, New York 381 p.

Lucifora, S., Cifelli, F., Rojay, B., Mattei, M. 2013. Paleomagnetic rotations in the Late Miocene sequence from the Çankırı Basin (Central Anatolia, Turkey): The role of strike–slip tectonics, Turkey. Journal of Earth Science 22, 778-792.

Lyatsky, H., Dietrich, J. 1998. Mapping Precambrien Basement Structure Beneath The Williston Basin in Canada: Insights From Horizontal-Gradient Vector Processing of Gravity and Magnetic Data. Canadian Journal of Exploration Geophysics 34 (1&2), 40-48.

Miller, H., Singh, V. 1994. Potential field tilt-a new concept for location of potential field sources. Journal of Applied Geophysics 32, 213-217.

MTA. 2002. 1/500.000 ölçekli Türkiye Jeoloji Haritası, Kayseri Paftası. Maden Tetkik ve Arama Genel Müdürlüğü, Ankara.

Nairn, S.P., Robertson, A.H.F., Ünlügenç, U.C., Taşlı, K, İnan, N. 2013. Tectonostratigraphic evolution of the Upper Cretaceous-Cenozoic central Anatolian basins: an integrated study of diachronous ocean basin closure and continental collision. Geological Development of Anatolia and the Easternmost Mediterranean Region. Geological Society, London Special Publication 372, 343-384.

Naumann, E. 1896. Die Grundlinien Anatoliens und Centralasiens. Geographische Zeitschrift 2(1), 7-25.

Okay, A., Tüysüz, O. 1999. Tethyan sutures of northern Turkey. Geological Society, London, Special Publication 156, 475-515.

Oruç, B. 2011. Edge Detection and depth estimation using a tilt angle map from gravity gradient data of the Kozaklı-Central Anatolia region, Turkey. Pure and Applied Geophysics 168, 1769-1780.

Oruç, B. 2013. Yeraltı Kaynak Aramalarında Gravite Yöntemi. Umuttepe Yayınları 270, Kocaeli.

Özsayın, E., Dirik, K. 2007. Quaternary activity of the Cihanbeyli and Yeniceoba Fault Zones: İnönü-

Eskişehir Fault System, central Anatolia. Turkish Journal of Earth Sciences 16, 471-492.

Özsayın, E., Çiner, A., Rojay, B., Dirik, K., Melnick, D., Fernando-Blanco, D., Sudo, M. 2013. Plio-Quaternary extensional tectonics of the Central Anatolian Plateau: A case study from the Tuz Gölü Basin, Turkey. Turkish Journal of Earth Science 22,5, 691-714.

Pınar, R. 1984. Potansiyel Alanlarda Yukarı ve Aşağı Analitik Uzanımlar. Bilimsel Madencilik Dergisi 23(2), 5-18.

Pick, M., Picha, J., Vyskocil, V. 1973. Theory of the Earth's Gravity Field. Elsevier, Amsterdam 538 p.

Platzman, E. S., Tapırdamaz, C., Sanver, M. 1998. Neogene anticlockwise rotation of central Anatolia (Turkey): Preliminary paleomagnetic and geochronological results. Tectonophysics 299, 175–189.

Poisson, A., Guezou, J.C., Öztürk, A., Inan, S., Temiz, H., Gürsoy, H., Kavak, K.S., Özden, S. 1996. Tectonic setting and evolution of the Sivas basin. International Geology Review 38, 833-853.

Reynolds, J.M. 2011. An Introduction to Applied and Environmental Geophysics, 2nd Edition. Wiley&Blackwell 710 p.

Rigo de Righi, M., Cortesini, A. 1960. Regional studies, Central Anatolian Basins progress report. Turkish Gulf Oil Co Rapor No II/11-12 (unpublished).

Roest, W., Verhoef, J., Pilkington, M. 1992. Magnetic Interpretation Using The 3-D analytic signal. Geophysics 57(1), 116-125.

Rojay, B. 2013. Tectonic evolution of the Cretaceous Ankara Ophiolitic Mélange during the Late Cretaceous to pre-Miocene interval in Central Anatolia, Turkey. Journal of Geodynamics 65, 66-81.

Saad, A. 2006. Understanding gravity gradients a tutorial. The Leading Edge 25(8), 942-949.

Salem, A., Williams, S., Fairhead, D., Smith, R., Ravat, D. 2008. Interpretation of magnetic data using tilt-angle derivatives. Geophysics 73(1), 14JF-Z11.

Schmitt, A.K., Danışık, M., Aydar, E., Şen, E., Ulusoy, İ., Lovera, O.M. 2014. Identifying the Volcanic Eruption Depicted in a Neolithic Painting at Çatalhöyük, Central Anatolia, Turkey. PLOS ONE 9(1): e84711.

Seyitoğlu, G., Kazancı, N., Karadenizli, L., Şen, Ş., Varol, B., Karabıyıkoğlu, T. 2000. Rockfall avalanche deposits associated with normal faulting in the NW of Çankırı basin: implication for the post-collisional tectonic evolution of the Neo-Tethyan suture zone. Terra Nova 12, 245-251.

Seyitoğlu, G., Işık, V., Gürbüz, E., Gürbüz, A. 2017. The discovery of a low-angle normal fault in the Taurus Mountains the İvriz detachment and implications concerning the Cenozoic geology of southern Turkey. Turkish Journal of Earth Sciences 26, 189-205.

Seymen, İ. 1984. Kırşehir masifi metamorfitlerinin jeoloji evrimi. Ketin Sempozyumu, Türkiye Jeoloji Kurumu Yayını 133-48.

Soengkono, S. 1999. Te Kopia geothermal system (New Zeland)-the relationship between its structure and extent. Geothermics 28(6), 767-784.

Şaroğlu, F., Emre, Ö., Boray, A. 1987. Türkiye'nin diri fayları ve depremsellikleri. Maden Tetkik ve Arama Genel Müdürlüğü Rapor No: 8174, 394 s. Ankara (unpublished).

Şengör, A., Yılmaz, Y. 1981. Tethyan evolution of Turkey: A plate tectonic approach. Tectonophysics 75, 181-241.

Tatar, O., Piper, J.D.A., Gürsoy, H., Temiz, H. 1996. Regional significance of neotectonic counterclockwise rotation in central Turkey. International Geology Review 38, 692-700.

Telford, W.M., Geldart, L. P., Sheriff, R.E., Keys, D.A. 1990. Applied Geophysics, 2nd Edition. Cambridge University Press, Cambridge 770 p.

Toprak, V. 2003. Tuzgölü Fay kuşağı Hasandağ kesiminin özellikleri. Türkiye Petrol Jeologları Derneği Özel Sayı 5, 71-84.

Toprak, V., Göncüoğlu, M.C. 1993. Tectonic control on the development of the Neogene-Quaternary Central Anatolian Volcanic Province, Turkey. Geological Journal 28, 357-369.

Turgut, S. 1978. Tuz Gölü havzasının stratigrafik ve çökelsel gelişimi: Türkiye IV. Petrol Kongresi Bildirileri 115-126 p.

Tüysüz, O., Dellaloğlu, A.A., Terzioğlu, N. 1995. A magmatic belt within the Neo-Tethyan suture zone and its role in the tectonic evolution of northern Turkey. Tectonophysics 243, 173–191.

Uğurtaş, G. 1975. Geophysical Interpretation of Part of The Tuz Gölü Basin. Bulletin of the Mineral Research and Exploration 85, 38-45.

Ulu, Ü., Öcal, H., Bulduk, A., Karakaş, M., Arbas, A., Saçlı, L., Karabıyıkoğlu, M. 1994. Cihanbeyli-Karapınar yöresi geç Senozoyik çökelme sistemi: Tektonik ve iklimsel önemi. Türkiye Jeoloji Kurumu Bülteni 9, 149-163.

Uygun, A., Yaşar, M., Erkan, M., Baş, H., Çelik, E., Aygün, M., Ayok, F. 1982. Tuzgölü havzası projesi, Cilt 2. Maden Tetkik ve Arama Genel Müdürlüğü Rapor No:6859, Ankara, (unpublished).

Ünalan, G., Yüksel, V. 1978. Eski Bir Graben Örneği: Haymana-Polatlı Havzası. Türkiye Jeoloji Bülteni 21, 165-169.

Verduzco, B., Fairhead, J.D., Green, C.M., Mackenzie, C. 2004. New insights into magnetic derivatives for structural mapping. The Leading Edge 23(2), 116-119.

Whitney, D.L., Teyssier, C., Dilek, Y., Fayon, A.K. 2001. Metamorphism of the Central Anatolian Crystalline Complex, Turkey: influence of orogen-normal collision vs wrench-dominated tectonics on P-T-t paths. Journal of Metamorphic Geology 19, 411-432.

Wilcox, L. 1974. An analysis of Gravity Prediction Methods For Continental Areas. Defense Mapping Agency Aerospace Center, Publication No. 74-001.

Yalınız, M.K., Floyd, P.A., Göncüoğlu, M.C. 2000. Petrology and geotectonic significance of plagiogranite from the Sarikaraman ophiolite (Central Anatolia, Turkey). Ofioliti 25, 31-37.

Yıldırım, C. 2014. Relative tectonic activity assessment of the Tuz Gölü Fault Zone; Central Anatolia, Turkey. Tectonophysics 630, 183-192.

Yüksel, S. 2011. Petrol Aramacılığında Doğal Potansiyel Yöntemler Gravite ve Manyetik. TPAO Kurum İçi Eğitim Notları 231 s.

Yürür, M.T., Genç, Y. 2006. The Savcili thrust fault (Kirsehir region, central Anatolia): a backthrust fault, a suture zone or a secondary fracture in an extensional regime? Geological Carpathica 57, 47-56.

Zhang, H., Tian-You, L., Yu-Shan, Y. 2011. Calculation of gravity and magnetic source boundaries based on anisotropy normalized variance. Chinese Journal of Geophysics 54(4), 560-567.